

ON THE CAPACITY OF UNDERLAY COGNITIVE
RADIO NETWORKS OVER GENERALIZED-K
COMPOSITE FADING CHANNELS

BY

MAJID HAMOUD KHOSHAFI

A Thesis Presented to the
DEANSHIP OF GRADUATE STUDIES

KING FAHD UNIVERSITY OF PETROLEUM & MINERALS

DHAHRAN, SAUDI ARABIA

In Partial Fulfillment of the
Requirements for the Degree of

MASTER OF SCIENCE

In

ELECTRICAL ENGINEERING


DECEMBER 2016

KING FAHD UNIVERSITY OF PETROLEUM & MINERALS
DHAHRAN 31261, SAUDI ARABIA

DEANSHIP OF GRADUATE STUDIES

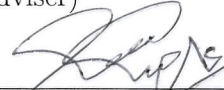
This thesis, written by **MAJID HAMOUD KHOSHAFI** under the direction of his thesis adviser and approved by his thesis committee, has been presented to and accepted by the Dean of Graduate Studies, in partial fulfillment of the requirements for the degree of **MASTER OF SCIENCE IN ELECTRICAL ENGINEERING**.

Thesis Committee

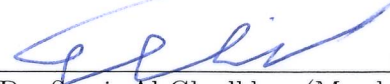


Dr. Saad Al-Ahmadi (Adviser)

(Co-adviser)



Dr. Ali Muqaibel (Member)

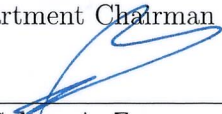


Dr. Samir Al-Ghadhban (Member)

(Member)



Dr. Ali A. Al-Shaikhi
Department Chairman



Dr. Salam A. Zummo
Dean of Graduate Studies



10/1/17
Date

©Majid Hamoud Khoshafa
2016

Dedication

To my parents, wife, children, brothers and sister for their endless support and love.

ACKNOWLEDGMENTS

All praise and thanks be to Almighty Allah, the one and only who helps us in every aspect of our lives.

Acknowledgement is due to King Fahd University of Petroleum and Minerals for giving me this precious opportunity to resume my Master degree.

I would like to express deep gratefulness and appreciation to my Thesis advisor Dr. Saad Al-Ahmadi for his continuous help, guidance, and encouragement throughout the course of this work. He spent a lot of his precious time helping me and advising me at each step.

Additionally, I would like also to thank my Thesis committee members: Dr. Samir Al-Ghadhban and Dr. Ali Muqaibel for their great help and cooperation, which contributed significantly to the improvement of this work.

Finally, my heartfelt gratitude goes to my parents, wife, children , brothers and sister for their encouragement, prayers, and moral support.

TABLE OF CONTENTS

ACKNOWLEDGMENTS	iii
LIST OF TABLES	viii
LIST OF FIGURES	ix
LIST OF ABBREVIATIONS	xi
LIST OF SYMBOLS	xiii
ABSTRACT (ENGLISH)	xv
ABSTRACT (ARABIC)	xvii
CHAPTER 1 INTRODUCTION	1
1.1 Introduction	1
1.2 Thesis Motivation	3
1.3 Thesis Contributions	5
1.4 Thesis Organization	7
CHAPTER 2 BACKGROUND AND LITERATURE REVIEW	8
2.1 Background	8
2.1.1 Scarcity of Spectrum Resources	9
2.1.2 Cognitive Radio Networks	10
2.1.3 Fading Channels	17
2.1.4 Generalized-K Composite Fading Model	21

2.1.5	Performance Metrics	23
2.1.6	Power Constraints	26
2.2	Literature Review	26
2.2.1	Cognitive Radio Networks	27
2.2.2	Capacity and Power Constraints	28
2.2.3	MIMO Cognitive Radio Networks	30
2.2.4	Relaying in Cognitive Radio Networks	31
 CHAPTER 3 CAPACITY OF CR WITH SINGLE PU		34
3.1	Introduction	34
3.2	System Model-Single PU	35
3.3	Ergodic Capacity	36
3.3.1	Ergodic Capacity Under Average Received-Power Constraint	36
3.3.2	Ergodic Capacity over Nakagami Fading Channel	43
3.3.3	Ergodic Capacity Under Peak Received-Power Constraint	44
3.4	Outage Probability	46
3.4.1	Outage Probability Under Average-Power Constraints	46
3.4.2	Outage Probability Under Peak Received-Power Constraint	49
3.5	Results and Discussions	50
3.5.1	Ergodic Capacity	50
3.5.2	Outage Probability	55
3.6	Conclusions	57
 CHAPTER 4 CAPACITY ANALYSIS OF CR WITH MULTIPLE PRIMARY USERS		59
4.1	Introduction	59
4.2	System and Channel Models	61
4.3	Capacity of CR Network with Multiple Primary Users	62
4.3.1	Ergodic Capacity	63
4.3.2	Outage Probability	65
4.4	Results and Discussions	66

4.5	Conclusions	68
CHAPTER 5 CAPACITY OF UNDERLAY MULTIHOP COGNITIVE RELAYING		69
5.1	Introduction	69
5.1.1	System and Channel Model	70
5.2	Ergodic Capacity	73
5.3	Outage Probability	75
5.4	Results and Discussion	76
5.5	Conclusions	78
CHAPTER 6 CONCLUSIONS AND FUTURE WORK		81
6.1	Conclusions	81
6.1.1	Capacity of SU with Single PU	81
6.1.2	Capacity of SU with Multiple PUs	82
6.1.3	Capacity of Cognitive Multihop Relaying	83
6.2	Future Work	83
APPENDICES		86
APPENDIX A		86
A.1	Ergodic Capacity - Single PU	86
A.2	Outage Probability - Single PU	88
APPENDIX B		89
B.1	PDF Derivations - Multiple PUs	89
APPENDIX C		92
C.1	PDF Derivations - Multihop Relaying	92
REFERENCES		93
VITAE		104

LIST OF TABLES

2.1	Spectrum utilization [1]	10
-----	------------------------------------	----

LIST OF FIGURES

2.1	Spectrum usage [2].	9
2.2	Spectrum sharing paradigms [3].	13
2.3	Architecture of cognitive radio network [4].	15
2.4	Cognitive radio applications [5].	16
3.1	System model - Single PU.	35
3.2	The Monte-Carlo simulation and analytical plots for the $f(\chi)$ of Rayleigh multipath fading channels with heavy shadowing	41
3.3	The Monte-Carlo simulation and analytical plots for the $f(\chi)$ of Rayleigh multipath fading with moderate shadowing.	42
3.4	The ergodic capacity of the SU for several Nakagami fading scenarios.	51
3.5	Ergodic capacity of SU for different composite fading scenarios. .	52
3.6	Ergodic capacity of SU for different composite fading scenarios for $Q_{av} = Q_{peak} = Q$	53
3.7	Ergodic capacity of SU for different composite fading scenarios. .	54
3.8	Ergodic capacity for both exact and approximation cases.	55
3.9	Outage probability of generalized-K Composite fading channel for Q_{av}	56
3.10	Outage probability of SU for different composite fading scenarios.	57
4.1	System model- multiple PUs.	61
4.2	Monte-Carlo simulations and analytical results for the $f(\chi)$ of Rayleigh multipath fading with heavy shadowing for different n . .	64
4.3	Ergodic capacity of SU vs Q_{peak}	66

4.4	The outage probability of the SU with multiple PUs vs Q_{peak} with heavy and moderate shadowing Rayleigh fading channels for the SU.	67
5.1	System model- multihop cognitive relaying.	71
5.2	Analytical and Monte-Carlo simulation plots for the PDF $f(x)$ of multihop cognitive relaying over composite fading channels for $m_{ms} = m_{mp} = 1, m_{ss} = m_{sp} = 2, N = 2, 3$	73
5.3	Ergodic capacity versus Q_{peak} for $N = 2, 4$	77
5.4	The ergodic capacity vs Q_{peak} for different fading and shadowing conditions, $N = 3$	78
5.5	The outage probability verse Q_{peak} for different number of relays.	79
5.6	The outage probability verse Q_{peak} for different fading conditions and $m_{ms} = m_{mp} = 1, m_{sp} = 0.5, N = 3$	80

LIST OF ABBREVIATIONS

AF	Amplify-and-Forward
AWGN	Additive White Gaussian Noise
BER	Bit Error Rate
BS	Base Station
CB	Cognitive Beamforming
CDF	Cumulative Distribution Function
CR	Cognitive Radio
CSI	Channel State Information
DE	Decode-and-Forward
DSA	Dynamic Spectrum Access
EIC	Effective Interference Channel
FCC	Federal Communications Commission
FDM	Frequency Division Multiplexing
i.i.d.	Independent and Identical Distribution
i.n.d.	Independent and Non-identical Distribution
LOS	Line Of Sight
MGF	Moment Generating Function
MIMO	Multiple Input Multiple Output
MRC	Maximal-Ratio Combining
PDF	Probability Density Function
PU	Primary User
QoS	Quality of Service
RV	Random Variable
SC	Selection Combining
SE	Spectral Efficiency

SIR	Signal to Interference Ratio
SNR	Signal to Noise Ratio
SU	Secondary User
TAS	Transmitted Antenna Selection
UWB	Ultra Wide Band

LIST OF SYMBOLS

$E[.]$	expectation operator
$[.]^+$	$\max(.,0)$
$F_X(x)$	CDF of the RV X
$H(x)$	Fox H-function
$G(x)$	Meijer G-function
${}_2F_1(\cdot)$	Gauss hypergeometric function
C	ergodic capacity
$f_X(x)$	PDF of the RV X
P	signal power
B	channel bandwidth
h	channel coefficient
γ	signal to noise ratio (SNR)
N_o	power spectral density of AWGN noise
Ω	local power
g	power channel gain
$\Gamma(\cdot)$	Gamma function
σ_s	the dB-spread
m_s	shadowing severity
$K_v(\cdot)$	Modified Bessel function of the second kind and order v
ϵ	adjustment factor
Q_{peak}	peak power threshold
Q_{av}	average power threshold
$Pr\{A\}$	Probability of A
g_s	primary users power channel gain
g_p	secondary user power channel gain

λ_0	lagrangian multiplier
$\beta(.,.)$	Beta function
$P_{out}(.)$	outage probability
R	target rate
n	number of PUs
N	number of intermediate relays
γ_{e2e}	the end-to-end SNR
γ_k	instantaneous SNR
γ_{e2e}^{up}	upper-bound SNR
C^{up}	upper-bound ergodic capacity
P_{out}^l	lower-bound outage probability

THESIS ABSTRACT

NAME: Majid Hamoud Khoshafa
TITLE OF STUDY: On the Capacity of Underlay Cognitive Radio Networks
over Generalized-K Composite Fading Channels
MAJOR FIELD: Electrical Engineering
DATE OF DEGREE: December 2016

Due to the rapid evolution of wireless communications technology, radio spectrum is rapidly becoming one of the most precious resources on our planet. Spectrum scarcity is considered as a significant challenge for future wireless communication systems. According to the recent studies, the allocated radio spectrum is not efficiently exploited together with the increasing demand for high data rate wireless services. Based on this, cognitive radio (CR) has been proposed to cope with both the under-utilization and scarcity of the radio spectrum. The main purpose of CR is to permit the secondary users (SUs), unlicensed users, to share the radio spectrum of the primary users (PUs), licensed users, which enhances the utilization of the radio spectrum. On the other hand, the performance of the PUs should not be affected by the interference caused by the SUs. Thus, the interference must

not exceed a predetermined threshold.

The aim of this thesis is to analyze the capacity of underlay cognitive radio networks in terms of two relevant performance metrics, namely the outage probability and the ergodic capacity over generalized-K composite fading channels for three particular scenarios for CR systems. The first scenario considers a single PU with two SUs in which both average and peak received power constraints are taken into account. Closed-form expressions for the two performance metrics, the ergodic capacity and the outage probability, are derived. To gain more insights, two interesting cases for different shadowing scenarios are studied in details. In the second part of this thesis, the performance of CR networks is examined under the peak power constraints for multiple primary users where closed-form expressions for both the heavy and moderate shadowing scenarios are derived. In addition, the effect of the number of PUs on the performance metrics is revealed. In the final part of this thesis, the capacity of underlay cognitive multihop relaying is investigated over generalized-K fading channels. In doing so, we derive upper bound expression for both the ergodic capacity and the lower bound expression for outage probability of the SU. Using both expressions, new insights in the performance of the cognitive multihop amplify-and-forward (AF) relaying are revealed. Finally, for all parts in this thesis, the derived expressions and the obtained results are verified by Monte-Carlo simulations.

ملخص الأطروحة

الأسم
عنوان الأطروحة
القسم
التاريخ

ماجد حمود خشافه
دراسة أداء الشبكات الراديوية الإدراكية من حيث السعة عبر قنوات التلاشي و التظليل
الهندسة الكهربائية
ديسمبر 2016

نظرًا إلى التطور السريع في تكنولوجيا الإتصالات اللاسلكية، سرعان ما أصبح الطيف الراديوي واحد من أتمن الموارد في كوكبنا. تعتبر ندرة الطيف الراديوي من أهم التحديات التي تواجهها أنظمة الإتصالات اللاسلكية. ووفقا للدراسات الحديثة فهناك عدم إستغلال للطيف الراديوي بكفاءة عالية مصاحباً للطلب المتزايد على الخدمات اللاسلكية مثل زيادة معدل سرعة نقل البيانات. فقد تم إقتراح الشبكات الراديوية الإدراكية (Cognitive Radio Networks) للتغلب على مشاكل ندرة الطيف الراديوي وعدم الإستغلال الأمثل له. الفكرة الأساسية لعمل هذه الشبكات تقوم أساس السماع للمستخدمين الغير مرخص لهم باستخدام حزمة معينة من الطيف الراديوي ومشاركة تلك الحزمة مع المشتركين المرخص لهم استخدامها بشرط عدم الإضرار بالمستخدمين الأساسيين. لذلك يجب ان يكون مقدار التداخل الناتج عن المستخدمين الثانويين ضمن قيمة محددة مسبقاً لا يتم تجاوزها. لهذا تعتبر الشبكات الراديوية الإدراكية ذات أهمية كبيرة لأنظمة الإتصالات الحالية والمستقبلية.

الهدف من هذه الأطروحة هو دراسة أداء الشبكات الراديوية الإدراكية من حيث السعة (Ergodic Capacity) و إحتمالية القطع (Outage Probability) عبر قنوات التلاشي من نوع (Generalized-K Composite Fading Channels). وقد تم العمل في هذه الأطروحة على ثلاثة سيناريوهات في الشبكات الراديوية الإدراكية. النوع الأول يتألف من مستخدم أساسي واحد و مستخدمين ثانويين هما المرسل و المستقبل. من خلال النظر في التداخل الناتج من المستخدم الثانوي، فإن هناك نوعين من قيود الطاقة سيتم أخذهما بعين الإعتبار في عمليات التحليل الرياضي. وقد تم إستنتاج صيغ جبرية لأداء تلك الشبكات في هذا السيناريو. أما بالنسبة إلى النوع الثاني، فإنه يتألف من عدد من المستخدمين الأساسيين بالإضافة الى مستخدمين ثانويين المرسل والمستقبل. لمعرفة المزيد من تأثير التظليل و التلاشي على أداء الشبكات في هذا السيناريو، فقد تم اشتقاق الصيغ الجبرية و التأكد من دقتها. في الجزء الاخير من هذه الأطروحة، تمت دراسة وتحليل أداء الشبكات الراديوية الإدراكية عبر إستخدام المرحلات المتعددة. فقد تم إستنتاج الصيغة الجبرية ذات الحد الأعلى للسعة و الصيغة الجبرية ذات الحد الأدنى لإحتمالية القطع. تم بإستخدام هذه الصيغ الكشف عن معلومات جديدة توضح أداء الشبكات الراديوية الإدراكية ذات المرحلات المتعددة و التأثير المتبادل لكلاً من التظليل و التلاشي عليها. و قد تم

ايضاً رسم وتوضيح كلاً من النتائج المحددة و النتائج الدقيقة لغرض المقارنة. إضافة الى ذلك فقد تم التأكد من صحة جميع الصيغ التحليلية المشتقة و النتائج المكتسبة لجميع السيناريوهات في هذه الأطروحة بواسطة مونت كارلو للمحاكاة الحاسوبية.

CHAPTER 1

INTRODUCTION

1.1 Introduction

Recently, there has been witnessed a dramatic development of wireless communication technologies which has led to more scarcity of spectrum resources. In order to utilize the available spectrum efficiently, spectrum usage strategies were extensively investigated by researchers to overcome the issue of spectrum scarcity. Cognitive radio (CR) was proposed as one of the candidate schemes to cope with the issue of spectrum deficiency[6].

CR networks can be defined as intelligent wireless networks which can adapt to their environment, so they can dynamically regulate their parameters such as frequencies, waveforms, and protocols to efficiently access the shared spectrum band. In CR networks, the users are classified into primary users (PUs) and secondary users (SUs). The PUs are the licensed users and they have priority in utilizing the specific spectrum band. However, the SUs are allowed, using a

certain protocol, to share the spectrum with the PUs [7].

The capacity of CR networks has received attention as the main metric which is utilized to quantify the performance of the CR networks. In wireless channels, the radio wave propagation is experienced by many factors like small-scale fading (multipath) and large-scale fading (shadowing). For the multipath fading, the channel is described by various models based on the radio propagation environment such as the Rayleigh model for non-line-of-sight (NLOS) channels, the Nakagami or Rician models for LOS channels, and the Lognormal or Gamma models for shadowing. However, wireless channels might be jointly affected by both multipath and shadowing. This phenomenon can be seen in some scenarios such as the congested urban areas with slow mobility and for geographically distributed receivers. Thus, the generalized-K composite fading model was proposed to model this phenomenon [8]. The aim of this thesis is to investigate and analyze both outage probability and ergodic capacity of an underlay CR networks under received-power constraints over generalized-K composite fading channels. In this thesis, closed-form expressions for both the outage probability and the ergodic capacity of an underlay CR are derived for different scenarios. The thesis consists of three different frameworks of CR settings: CR with single PU, CR with multiple PUs, and CR with multihop relaying. Furthermore, the results are compared with unshadowed Rayleigh channels and the analytical results are verified by Mont-Carlo simulations for different fading scenarios.

1.2 Thesis Motivation

In this section, we discuss the main motivations that lead to this thesis work and how they are important to the area of research in CR networks.

Over the last few decades, wireless communication services have been rapidly growing that has produced considerable changes in several aspects of our life. As a result, wireless communications have become an essential part of mankind life throughout the world. Despite many wireless systems have been successfully used such as satellite systems, television broadcasting, mobile cellular systems, and wireless local area networks, various challenges have been risen for wireless communication systems. The efficient use of the inadequate frequency resources (spectrum scarcity) is considered as one of the crucial challenges in wireless communications. The evolution of new wireless applications, as well as the increasing demands on higher data rates of different wireless communication services, have driven to a significant lack of radio frequency bands. However, allocated spectrum bands are not well used. On the report of Federal Communications Commission (FCC) [9], the specified frequency bands are not utilized efficiently. Thus, spectrum scarcity is a very important issue in current and future wireless networks. Cognitive radio (CR) was proposed in [6] as a candidate scheme that has been put forward as a promising technology for future wireless communication.

The performance of an underlay cognitive systems is of a great interest to present insights on designing modern wireless communication networks. As can be seen from the open literature, the capacity of CR networks was extensively

discussed and evaluated by researchers over several fading channel models under different received power constraints. However, the capacity of the SU can be increased by taking the advantages of the fading effect between the SU transmitter (SU-Tx) and the PU receiver (PU-Rx). Furthermore, recently, the generalized-K composite fading model received interest as a tractable model used to analyze the capacity of the CR networks.

Motivated by the considerable importance of analyzing CR capacity over fading channels, in this thesis, three different scenarios of cognitive systems are presented. In the first scenario, the capacity of the cognitive radio networks is studied for single PU over generalized-K composite fading channels for both peak and average power constraints. In the second scenario, the same analysis is applied with multiple PUs. Finally, the performance analysis is investigated and evaluated for the cognitive multihop relaying scheme.

1.3 Thesis Contributions

The main contributions of this thesis work are briefly discussed in this section .

- The capacity of an underlay cognitive radio networks is studied over generalized-K composite multipath fading and shadowing channels while taking the peak and average power constraints into account where closed-form expressions are derived for both the outage probability and the ergodic capacity of the SU. The obtained results reveal new details on the joint effect of shadowing and the multipath fading on the capacity of the SU where the increase of the ergodic capacity and degradation of the outage probability are demonstrated and quantified. To gain more insights, two tractable and relevant composite fading scenarios, Rayleigh multipath fading with heavy and moderate shadowing are analyzed in details.
- The performance metrics of CR networks are examined under the peak power constraints with multiple PUs over two interesting scenarios, namely Rayleigh multipath fading channels with both heavy and moderate shadowing. To do so, the cumulative distribution function (CDF) and the probability density function (PDF) are derived. In particular, closed-form expressions are derived for both performance metrics for two interesting cases. More importantly, the obtained results reveal and quantify the effect of shadowing on performance of CR networks for different numbers of the multiple PUs. Moreover, the effect of the number of PU on the performance of CR networks is discussed. Furthermore, in order to evaluate the obtained

results, Mont-Carlo simulations are unitized to confirm the analytical expressions.

- Whereas the CR capacity has been well studied in the open literature, to the best of our knowledge, none of the previous work has investigated the ergodic capacity and outage probability for underlay CR networks in amplify-and-forward (AF) multihop relaying over independent and nonidentical distribution (i.n.d.) generalized-K shadowed multipath fading channels. In this thesis, we analyze both of these performance metrics to gain more insight into the combined effects of shadowing and multipath fading on the performance of the underlay CR networks. To do so, the PDF of end-to-end SNR is derived for this scenario. In this respect, the PDF expression is utilized to derive lower and upper bound expressions for both the outage probability and ergodic capacity, respectively. Interestingly, the obtained results provide interesting details on the joint effect of shadowing and multipath fading on the capacity of the SU in relay-assisted underlay CR networks. Furthermore, the analytical results are verified by Mont-Carlo simulations for different fading scenarios. For comparison purposes, the exact results using simulations are utilized to compare with the upper and lower bound results.

1.4 Thesis Organization

The purpose of this thesis is to analyze the performance of underlay CR networks over generalized-K composite fading channels. This thesis is prepared as the following; Chapter Two presents the background of cognitive radio networks, fading channels, channel capacity, and the generalized-K composite fading model considered in this thesis. The chapter also presents a literature review related to the capacity of CR networks over fading channels. Chapter Three presents the first scenario considered in this thesis. This chapter provides a comprehensive analysis of underlay cognitive networks with single PU in terms of the ergodic capacity and the outage probability. Chapter Four shows the second scenario studied in the thesis. In this chapter, the CR capacity analysis with multiple PUs is investigated. Chapter Five presents the third system model analyzed in this work. In this chapter, multihop cognitive relaying is analyzed for both ergodic capacity and outage probability. In addition, the upper bound PDF of end-to-end SNR is derived. Furthermore, tight formulas are derived for the performance metrics. Finally, Chapter Six concludes the thesis work by highlighting the main contributions and conclusions of the thesis. It also proposes future work on the relaying and multiple-input and multiple-output (MIMO) CR networks.

CHAPTER 2

BACKGROUND AND LITERATURE REVIEW

2.1 Background

In this section, the background of topics related to the thesis work is discussed. The scarcity of spectrum resources problem is investigated and CR networks are discussed in details. In addition, channel capacity is introduced. Moreover, fading channels are explored as the main problem in wireless communication systems. Furthermore, the generalized-K composite fading channel is described in details as the main channel model used in this work. Finally, a brief literature review is introduced.

2.1.1 Scarcity of Spectrum Resources

The increasing demand for high data rate multimedia applications and services has motivated researching spectrum efficient schemes that allow optimal utilization of the allocated electromagnetic spectrum. According to the Federal Communications Commission (FCC) [9], the assigned frequency bands are not efficiently utilized. Spectrum scarcity is a very important issue in current and future wireless networks. Furthermore, the use of the spectrum is regulated, hence, a lot of services and applications can be used in specific spectrum band without interference. However, there is no more

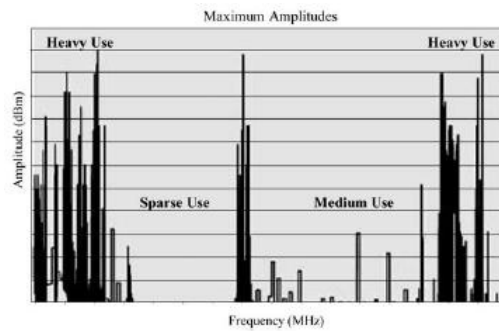


Figure 2.1: Spectrum usage [2].

available spectrum for the fast growth of wireless communications services [7]. In addition, a lot of studies showed that the spectrum is not utilized effectively as shown in Fig. 2.1. A study was made in Chicago, 2005 to measure the spectrum utilization for two days measurements period. The results illustrated that about 17.4% of the allocated spectrum was only used [10]. Moreover, another study was done in 2009 to measure the utilization of the licensed spectrum radio bands from 0.1 GHz up to 3 GHz [1] as shown

Table 2.1: Spectrum utilization [1]

System	Frequency [MHz]	Utilization [%]
TETRA	380–385/390–395	37.5
CDMA 1	410.2–412.8/420.2–422.8	50.7
CDMA 2	451.5–455.54/461.5–465.54	47.2
TV	470–862	20.4
E-GSM	888–915/933–960	51.9
GSM 1800	1710–1785/1805–1880	21.8
UMTS TDD	1920–1980/2110–2170	3.8
ISM	2400–2483.5	1.0

in Table 2.1. The study concluded that the total radio spectrum utilization is lower than 6.96%.

These studies concluded that an advanced technology should be used to utilize the spectrum efficiently. As a result, CR network was proposed as one of the candidate schemes to cope with this issue [6].

2.1.2 Cognitive Radio Networks

The CR networks are of great interest for current and future wireless communications. They have been put forward as a promising technology for future wireless communication. Furthermore, CR networks have the ability to gather information about their surrounding environment, such as power, frequency, bandwidth, modulation, etc. Thus, they can reconfigure their parameters depending on interaction with their surrounding where they operate.

Cognitive Radio Characteristics

In CR schemes, the three main characteristics are reconfigurability, sensing, and learning and adaptability.

- **Reconfigurability**: the capability to adapt the operating parameters of the CR such as frequency, access method, modulation, etc., in real time to the variations of the radio environment [7].
- **Sensing**: the capability to detect the signals of the PU to find the spectrum holes and to measure interference from the surrounding environment. Sensing is very important to the CR network because the change in the operating parameters depends on the given information of the radio environment. There are many techniques that are used in the spectrum sensing like maximum eigenvalue technique, matched filter sensing, energy sensing, and cyclostationary sensing techniques. Furthermore, hybrid techniques which consist of the above methods are used to increase the performance of the detection [2].
- **Learning and adaptability**: the capability to recognize and analyze the given data to modify the operational parameters of the CR network according to the prior data [5].

CR Network Paradigms

The CR networks are classified into three paradigms [3]: underlay, interweave and overlay CR networks.

- **Underlay CR:** The underlay paradigm comprises techniques that permit communication of the SUs at the same time when the PUs are transmitting their signals too, taking in account that the amount of the interference caused by SUs is known as shown in 2.3 a. As a result, the power constraints are applied on SU-Tx to guarantee that the amount of the interference created by SU does not harm the PU. Spread spectrum techniques are used in this method, so the transmitted power by SU is spread over a large band of spectrum. In this part of the spectrum, the transmitted signals by SU is considered as a noise for the PU. Moreover, ultra wide band (UWB) can be employed in this approach. The UWB technology is particularly convenient for underlay spectrum sharing due to the spread of the SU's signal over a wide bandwidth. In both techniques, the transmitted signal of the SU should be below the interference threshold that the PU can tolerate. In the underlay spectrum sharing, the control of the transmitted power of the SU is much important than the detection of the PU to ensure that the amount of interference created by SU on the PU is less than a definite threshold. For this paradigm, the channel state information (CSI) of the interference channel between the SU-Tx and PU-Rx should be perfect for the SU [2].
- **Interweave CR:** The original idea for CR [6] was based on the interweave paradigm. It is an intelligent CR network that regularly mon-

itors the radio spectrum, effectively detects the spectrum holes, and then SUs can access to the spectrum as shown in 2.3 b. In doing so, sensing techniques are utilized to detect the existence of the PUs. Moreover, the frequency division multiplexing (FDM) technique is employed in this type. Furthermore, orthogonal (OFDM) is also used in interweave CR because the subcarrier transmission is provided by OFDM to transmit only the signal of the SU when the PU is absent [5].

- **Overlay CR:** In overlay paradigms, the SU-Tx has knowledge of the PUs codebooks as well as its messages. In this respect, the cognitive radio utilizes advanced coding and signal processing to enhance the quality of service (QoS) of PUs where the SUs act as relays for the PUs [3].

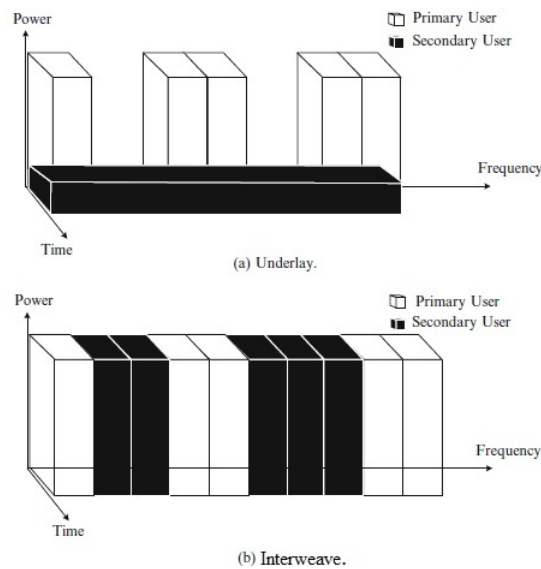


Figure 2.2: Spectrum sharing paradigms [3].

In this thesis, the underlay CR scheme is used because it is more simple than overlay and interweave schemes. Moreover, it efficiently uses the spectrum compared with the other schemes.

Cognitive Radio Network Architecture

As the technology of CR is developed, SUs who are not the licensed users can temporally use the unoccupied spectrum band owned by PUs. Thereby, the components of the CR network architecture comprise both secondary and primary networks as illustrated in Fig. 2.3. Moreover, the primary network is the licensed network that has a license to operate in a specific frequency band. In addition, it is composed of a set of PUs with an infrastructure. Moreover, the PUs are controlled by the primary base station (BS). On the contrary, the CR network is the secondary network that consists of a set of SUs with/without an infrastructure. Moreover, the CR base stations can be used to control the SUs [4].

As illustrated in Fig. 2.3, CR operates in two spectrum bands: licensed and unlicensed spectrum bands. The SUs have three various access methods which are a primary network, CR ad hoc access and CR network. The CR network access means that the SUs can connect to the CR BS by using unlicensed and licensed frequency bands. Moreover, SUs can establish a connection by using the ad hoc network. Furthermore, the primary network access can be used by SUs to access to the primary BS by using the licensed

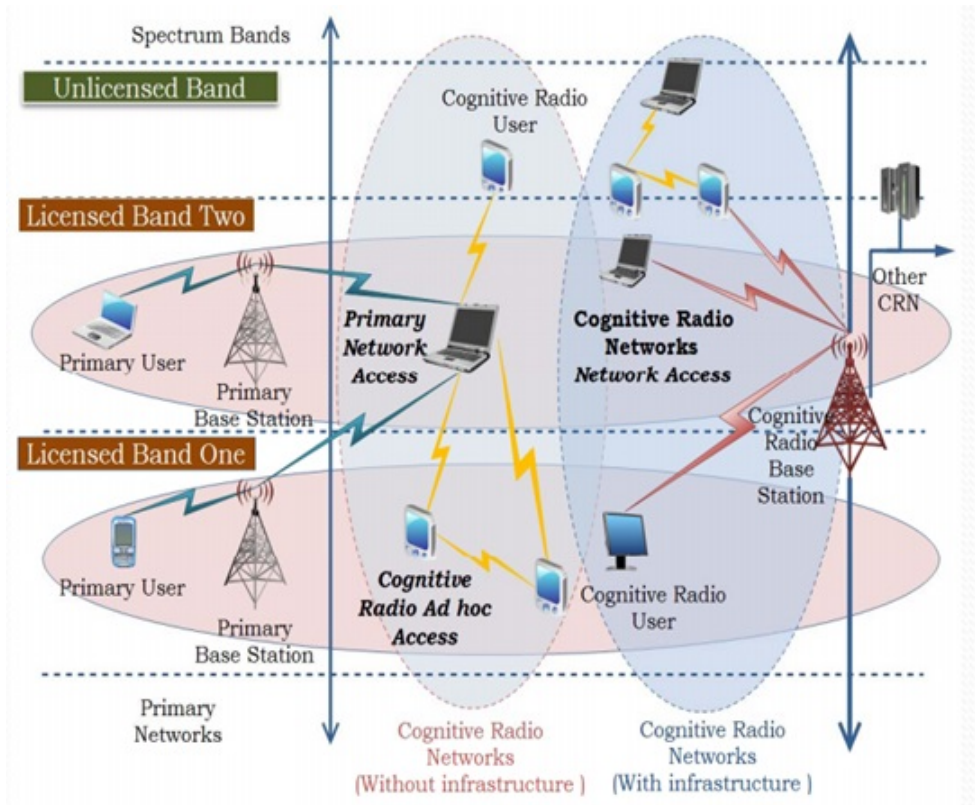


Figure 2.3: Architecture of cognitive radio network [4].

band [4].

Cognitive Radio Networks Applications

The key applications of the CR networks are the interoperability and the dynamic spectrum access (DSA) as shown in Fig. 2.4. CR schemes allow radios operating in various standards and protocols to establish communications among each other. This is called the interoperability. For instance, a CR scheme can establish a communication between several radio systems with different standards, protocols and carrier frequencies such as military and public safety networks. Due to the ability of CR network to reconfigure

its parameters to communicate with different communication systems employed in the field. Moreover, CR network is able to transmit in unoccupied radio spectrum whereas the licensed user is not affected by the interference; that is known as the DSA [5].

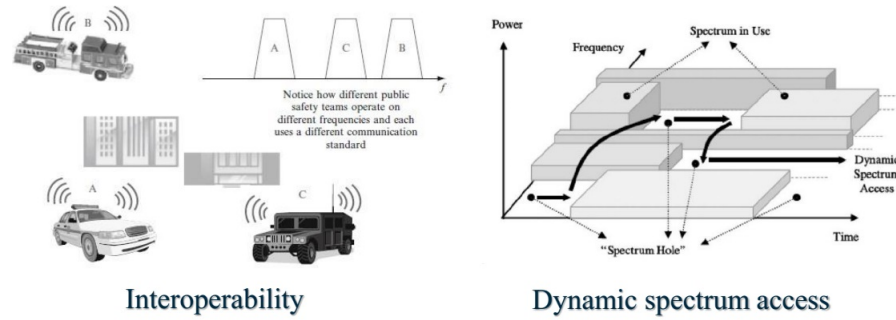


Figure 2.4: Cognitive radio applications [5].

Cognitive Radio Networks Challenges

The CR networks are used to cope with the issue of the spectrum scarcity but this benefit is gained at the expense of producing extra interference to the PUs. However, in the case of underlay CR networks, power constraints are applied to protect the PUs from the interference. In addition, for interweave CR network, the obtained information from the surrounding radio environment should be highly accurate to observe and detect the spectrum space. Furthermore, the sensing and learning processes are complex to implement.

2.1.3 Fading Channels

There are many characteristics that describe the fading channels in wireless communication systems. First of all, the envelope and phase fluctuation is one of the main characteristics of the fading channel. As a result of fading, the received signal changes in envelope and phase over the time duration. For non-coherent receivers, the phase fluctuation does not affect the system performance while it causes harm effects on the coherent receivers. Moreover, envelope fluctuation is very important for both systems [8]. Second, fast and slow fading depict the behavior of the channel according to the coherent time and the Doppler rate. Coherent time is defined as the time duration over which the received signals have a strong correlation while Doppler effects take place due to the fact that the receiver and the transmitting source are in motion relative to each other. Therefore, when the symbol duration of the signal is smaller than the coherence time, the fading is called slow fading; otherwise, it is called fast fading. Third, fading can be classified into frequency-selective fading and non-frequency-selective fading or flat fading. This classification depends on the coherence bandwidth which is defined as the range of frequency when two components of the frequency are highly correlated. In other words, if the transmitted bandwidth is larger than the coherence bandwidth, the channel is called frequency-selective channel; otherwise, it is called flat channel [11].

For the fading channel, the SNR is given by,

$$\gamma = \frac{P}{N_o B} |h|^2 \quad (2.1)$$

where γ is the SNR, P is the power of the signal, N_o is the power spectral density of AWGN noise, and h is the channel gain. The instantaneous capacity (C_o) of the fading channel is expressed as

$$C_o = B \log_2 \left(1 + \frac{P}{N_o B} |h_o|^2 \right) \quad (2.2)$$

where B is the channel bandwidth.

Rayleigh Multipath Fading Model

For multipath fading with non-line-of-sight (NLOS) channel, Rayleigh model is considerably used. In this model, the number of obstacles is large between the source and the destination in the propagation environment. Hence, the received signal in this model experiences high variations. However, due to the diffractions, reflections, and scattering, there are some propagation paths. The PDF of Rayleigh distribution is expressed as,

$$f_X(x) = \frac{x}{\sigma^2} \exp\left(\frac{-x^2}{2\sigma^2}\right), \quad x \geq 0, \quad (2.3)$$

However, the instantaneous SNR, γ , would be exponentially distributed,

$$f_\gamma(\gamma) = \frac{1}{\bar{\gamma}} \exp\left(-\frac{\gamma}{\bar{\gamma}}\right), \quad \gamma \geq 0, \quad (2.4)$$

where $\bar{\gamma}$ is the average SNR.

Nakagami Multipath Fading Model

Nakagami distribution can be used to model the random variation of the signal envelope in a multipath fading channel with two main parameters, multipath fading parameter m_m , and local power Ω . When Ω is unity, the PDF of Nakagami distribution is given by [12],

$$f_X(x) = \frac{2m_m^{m_m} x^{2m_m-1}}{\Gamma(m_m)} \exp(-m_m x^2), \quad m_m \geq \frac{1}{2}, \quad (2.5)$$

where $\Gamma(\cdot)$ denotes the gamma function which can be calculated as, $\Gamma(m_m) = \int_0^\infty t^{m_m-1} e^{-t} dt$. If the mutipath fading parameter m_m equals to unity, the distribution represents the Rayleigh model. As the value of m_m becomes higher, the fading channel becomes less severe. Furthermore, for the Nakagami model, γ is distributed as Gamma distribution [8],

$$f_\gamma(\gamma) = \frac{m_m^{m_m} \gamma^{m_m-1}}{(\bar{\gamma})^{m_m} \Gamma(m_m)} \exp\left(-\frac{m_m \gamma}{\bar{\gamma}}\right), \quad \gamma \geq 0, \quad (2.6)$$

Log-normal Shadowing Model

In terrestrial systems, the channel is affected by slow variation of the local-mean power owing to shadowing. Shadowing is caused by large obstacles affecting the wave propagation such as buildings, trees, and hills. According to the empirical measurements, the Log-normal distribution is good to model the shadowing. In addition, Log-normal shadowing is described by dB-spread that is related to the standard deviation σ_s . The dB-spread has typical ranges from 4 to 12 dB [11]. The PDF of Log-normal distribution is expressed as,

$$f_X(x) = \frac{1}{x \sigma_s \sqrt{2\pi}} \exp\left(-\frac{(\log(x) - \mu)^2}{2\sigma_s^2}\right), \quad x > 0, \quad (2.7)$$

where σ_s is the standard deviation of the shadowing and μ is the mean. However, the PDF in (2.7) is difficult to analyze. Thus, the Gamma model is used as an alternative of the Log-normal PDF because it has a good fit for shadowing measurements [13]. The Gamma PDF is given by,

$$f_\gamma(\gamma) = \frac{m_s^{m_s} \gamma^{m_s-1}}{(\bar{\gamma})^{m_s} \Gamma(m_s)} \exp\left(-\frac{m_s \gamma}{\bar{\gamma}}\right), \quad \gamma \geq 0, m_s > 0, \quad (2.8)$$

where m_s indicates the shadowing parameter. Similar to the m_m parameter, the severity of the shadowing decreases when the m_s increases. The moment matching can be used to determine the relationship between parameters of

Gamma model in (2.8) and Log-normal model in (2.7) as [14],

$$m_s = \frac{1}{\exp(\sigma_s/8.686)^2 - 1}$$

2.1.4 Generalized-K Composite Fading Model

In some wireless channels, the radio wave propagation is distinguished by the joint effect of multipath fading and shadowing. For analyzing this type of composite fading, the model should contain multipath fading in addition to shadowing. The composite fading is the key to precise modeling of some practical wireless channels such as congested areas with low mobility [8]. For this model, Nakagami distribution and Log-normal distribution are normally used to model the multipath fading and the shadowing, respectively. However, the Log-normal distribution is difficult for analysis. For this reason, there are not closed-form expressions of the performance measures by using Log-normal distribution. Therefore, the Gamma distribution was suggested to model the shadowing fading as it approximates the Log-normal distribution.

For composite fading models, other models are used such as Rayleigh-lognormal, and Rician-lognormal models. Rayleigh-lognormal model is suitable for NLOS links. However, it is intractable [15]. Furthermore, Rician-lognormal is proposed for LOS links. However, it is not tractable. In addition, Nakagami-lognormal model is suggested because Nakagami distribu-

tion is mathematically tractable and it is fit for both NLOS and LOS links. Nevertheless, this composite model is not tractable [16]. For the composite fading, the generalized-K (Gamma-Gamma) model is utilized. To model scattering in radar, the generalized-K model was proposed [17]. In this context, this model has received worthy attention in wireless communications literature. In [14], a new expression for the PDF of the signal-to-interference ratio (SIR) was derived for the generalized-K composite fading channel. In addition, the new expression was used to analyze the outage probability, and BER. The authors in [18] analyzed the performance of the wireless networks like outage probability, ergodic capacity, and BER over the generalized-K fading channels. Furthermore, the derived expressions were evaluated by using the generalized hypergeometric function [19]. In [20], the outage probability was analyzed over the generalized-K composite fading channels. However, the extended generalized-K distribution was proposed in [21] to derive the PDF, CDF and moment generating function (MGF) of the SIR. Furthermore, the gained results were utilized to investigate the outage probability in the interference-limited systems [22].

By using (2.6) and (2.8), the composite multipath/shadowing can be modeled by using the generalized-K distribution [23],

$$f_{\gamma}(x) = \frac{2}{\Gamma(m_s)\Gamma(m_m)} q^{m_s+m_m} x^{\left(\frac{m_s+m_m}{2}\right)-1} \times K_{m_s-m_m}(2q\sqrt{x}), \quad x > 0, m_s > 0, m_m \geq 0.5, \quad (2.9)$$

where $q = \sqrt{\frac{m_m m_s}{\Omega_0}}$, and $K_v(\cdot)$ indicates the modified Bessel function of the second kind and order v [24]. However, for the generalized-K model, it is analytically difficult for further derivations due to the special function that is involved in. Thus, an approximation method was developed in [23] to obtain more tractable expressions. By using moment matching method, Gamma model can be utilized to approximate the generalized-K composite model as $K(m_m, m_s, \Omega) \approx \text{Gamma}(\kappa, \Theta)$ which simplify the analysis. The parameters κ and Θ can be computed as [25],

$$\kappa = \frac{m_m m_s}{m_m + m_s + 1 - m_m m_s \epsilon} \quad \text{and} \quad \Theta = \frac{\Omega}{\kappa} \quad (2.10)$$

where ϵ represents an adjustment factor.

2.1.5 Performance Metrics

Many metrics have been used to evaluate the performance of CR networks such as ergodic capacity, outage probability, average bit error rate, and outage capacity. In this thesis, the two main metrics are the ergodic capacity and outage probability.

Channel Capacity

In wireless communication systems, it is very important to know the limits of the achievable data rate. As a result, the concept of channel capacity

evolved to determine these limits. In this context, the channel capacity can be defined as the maximum achievable data rate that can be gotten by the channel without an error [26]. The well-known formula of the channel capacity is known as Shannon's capacity formula [27]. Consequently, the channel capacity over an AWGN can be calculated by,

$$C = B \log_2 (1 + \gamma) \quad (2.11)$$

where B is the channel bandwidth, and γ is the SNR. The unit of the capacity is bit per second (bits/sec) for the binary system that is expressed by the subscript 2 in \log_2 . However, the channel capacity can be normalized by B and then the capacity is measured by bits/sec/Hz, usually known as the spectral efficiency (SE). To simplify the computation of the channel capacity, the Natural logarithm \log is used instead of \log_2 . For this reason, the channel capacity is measured in nats/sec/Hz.

In practice, the CSI denotes the properties of the channel at the communications link. From these properties, the effect of scattering, shadowing, interference, and fading can be known on the signal propagation from the transmitter to the receiver. Thus, CSI should be estimated at the receiver and then fed back to the transmitter. However, the wireless channel capacity relies on the CSI at both the transmitter and the receiver. Most importantly, one of the most advantages of perfect CSI is that the receiver and the transmitter adapt to the changing channel conditions [26].

Ergodic Capacity

The ergodic capacity can be defined as the maximum average data rate that can be transmitted over the channel with a low probability of error. Ergodic capacity is a suitable metric for delayed transmissions [26]. Hence, capacity is computed after averaging over all values of channel gain and picking the maximum of all these averages when the allocated power vary. In order to average over power channel gain (g), the CSI is needed and the capacity is expressed by [28],

$$C = \max_{P(g) \geq 0} \text{E} \left[\log \left(1 + \frac{P(g)g}{N_0B} \right) \right] \quad (2.12)$$

Outage Probability

The outage probability can be defined as the probability that a specific transmission rate, R , is not supported because of channel variations. It is used as a performance metric for real-time applications [26]. The outage probability for a target rate (R) can be express as [28],

$$P_{out}(R) = \Pr \left\{ \log \left(1 + \frac{g\gamma}{N_o} \right) < R \right\} \quad (2.13)$$

2.1.6 Power Constraints

To maintain the QoS of the PU, the capacity of the SU in CR networks is analyzed under different power constraints. Hence, the interference produced by the SU on the PU should not overtake a predetermined threshold. The power constraints are classified into long-term power and short-term constraints [29].

In short-term power constraints, there are two kinds of power constraints: peak received-power and peak transmitted-power constraints. In the former paradigm, the transmitted signal by the SU should be below a peak received-power threshold (Q_{peak}). In addition, this constraint describes the real-time systems. In the latter paradigm, the transmitted power by the SU should not exceed a peak transmitted-power threshold (P_{peak}).

For the long-term power constraints, the average power constraints are used. They are categorized into average received-power (Q_{av}) and average transmitted-power (P_{av}) constraints at the PU. The Q_{av} denotes the certain average received-power threshold and P_{av} represents the average transmit power. This constraint describes the systems with delay.

2.2 Literature Review

In this section, the literature review is introduced

2.2.1 Cognitive Radio Networks

The CR technology has received worthy interest as a new technology to utilize the radio spectrum effectively. In [6], CR was proposed to permit many users from different networks to share the spectrum. This purpose can be done by collecting information from the radio environment, so CR network can be adapt by changing its parameters based on that information. As a result, PUs and SUs can share the same spectrum to overcome the shortage of the electromagnetic spectrum and to improve the capacity.

By using spectrum sensing, CR network can get the necessary information about its radio environments. This technique is utilized to sense the holes in the spectrum and to discover the presence of the PUs. Therefore, Many papers have focused on the spectrum sensing techniques, for instance, energy detector is used to uncover an unknown signal by using energy detector [30]. Moreover, [31] studied the detection of the strange signals over fading channels. More important, a new technique is used in [32] for spectrum sensing which is the maximum eigenvalue method. This technique is appropriate for very much similar signals. Other methods such as matched filter detection and cyclostationary were used [33]. Energy detection is more popular than other methods because it has less complication. Consequently, it is used in cognitive networks for fast sensing. New methods are suggested by applying two-step sensing method to enhance the performance of the detection. [34] presented two-step energy detection for sensing the spectrum holes. On

the other hand, a hybrid method is used in [35] which consists of two-stage sensing scheme where the first step is energy detection and the next step is cyclostationary detection. This method improves and achieves the detection in a much lower time of spectrum sensing.

2.2.2 Capacity and Power Constraints

Spectral efficiency (SE) is used to enhance the performance of the cellular systems. It measures the efficient exploitation of the spectrum. For fading point-to-point channels, the ergodic capacity was studied under the different power constraints in [36]. The analysis was carried out for two scenarios: with perfect CSI at both transmitter and receiver, and with CSI only at the receiver.

For the link-level CR network scenario, the capacity was first analyzed in [37] under the received-power constraint, at the PU-Rx, for AWGN channels where the closed-form expressions were derived. However, the average received-power is assumed to be known for the system where the system has the ability to avoid the interference harm on the PU by decreasing the amount of the transmitted power from the SU. In [38], the ergodic capacity of CR networks was investigated in the fading environments. Closed-form expressions were derived for both the peak and average received-power constraints. Moreover, the CSI was supposed to be perfect and known at both the receiver and the transmitter. In addition, the ergodic capacity for the SU

was evaluated for various fading models such as lognormal shadowing model, Rayleigh, and Nakagami multipath fading models. The results showed that the capacity of the SU increases in more severe fading conditions. This is primarily because the SU-Tx can transmit with higher power when the interference channel between the PU-Rx and the SU-Tx is in deep fade. Furthermore, the derivations were extended to the multiple PUs scenario only for Rayleigh channels. For joint power constraints, the authors in [39] analyzed both the outage and ergodic capacities of SU under combinations of transmitted and received power constraints. To do so, the optimal power allocation was obtained for both outage and ergodic capacities for each case of the joint power constraint combination where Rayleigh, Nakagami, and lognormal fading models were used. The results showed that the effect of the peak power constraints is more strict than the average power constraints to increase the SU capacity in the fading environments. In this context, the authors in [40] provided closed-form expressions for the minimum rate, outage, and ergodic capacities on CR networks for the Rayleigh fading model. That work was done jointly under both peak and average power constraints and perfect CSI at SU's transmitter and receiver. However, the obtained results showed that the peak received-power constraint has not a substantial effect on the ergodic capacity when the average received-power constraint is applied. On the contrary, the outage capacity is actually affected by the peak power constraint. For extended system model, the PU transmitter was

added for the model in [41] and its interference effect on the SU receiver was investigated over Rayleigh fading channels.

For the system-level CR network, capacity was analyzed in [42] under the average received-power constraint. Furthermore, it was also studied for multiple PU-Rxs as well as SU-Txs. The results showed that the uplink capacity in the CR based central access network is large with a small number of PU-Rxs. Nevertheless, the capacity decreases rapidly when the number of the primary users increases.

2.2.3 MIMO Cognitive Radio Networks

For CR networks, the main goal is to increase the capacity of the SU, whereas saving the PU from the interference caused by the SU. Recently, a lot of studies have been focused on using multiple-input and multiple-output (MIMO) in CR networks. In [43], the fundamental limits for MIMO CR networks were analyzed for link level between single SU and PU. The authors in [44] presented three schemes for MIMO technology in CR when the SU-Tx has perfect, partial, or imperfect knowledge of CSI to the PU receiver. The optimal SU-link beamforming was analyzed for the three scenarios in MIMO CR networks. In another study [45], the PU receiver was designed with multi-antenna and the cognitive beamforming (CB) was used to overcome the imperfect CSI problem. The idea of effective interference channel (EIC), was utilized where the EIC can be estimated at SU transmitter by obser-

vation of the PU signals. The results showed that by using CB with EIC, the capacity of the SU can be improved. In this context, the limits of the capacity of CR networks was studied with imperfect CSI [46].

2.2.4 Relaying in Cognitive Radio Networks

The first three-terminal communication model was introduced in [47] to investigate the concept of relaying. For this model, the capacity was analyzed for feedback, degraded, and reversely degraded relay channels. Since then, the relaying concept has been used in wireless communication systems to present worthy improvements in the diversity as well as the capacity [48]. Furthermore, decode-and-forward (DF) as well as amplify-and-forward (AF) were recognized as the two main strategies that were introduced in [49] for wireless relay networks. Moreover, the former type is better for the relays that are near the receiver while the latter is better for the relays that are near the transmitter.

Relaying has received more attraction in the CR networks by minimizing the interference and choosing terminals that produce less interference on the PU. As a result, relaying improves the capacity of the SU [50]. In this context, the authors in [51] analyzed the capacity of the relaying model for the SU in the spectrum-shearing networks under the power constraints. In addition, closed-form expressions were derived for both outage and ergodic capacities in multipath and shadowing environments for the DF protocol.

The obtained results showed that how the capacity of the relay channel changes according to cognitive requirements as well as the fading terms.

For DF relay-assisted CR networks, the outage probability and the ergodic capacity of the SU were analyzed in [52] under the peak power constraint. Furthermore, the results showed that while the number of the relays increases, the outage probability decreases. Consequently, the ergodic capacity increases. The best selection relay scheme was used in [53] to analyze both outage and ergodic CR capacities over Nakagami multipath fading channels where closed-form expressions were derived. In addition, the results showed that the effect of interference link has less impact than the fading links on both capacities. In particular, the impact of the PU-Tx on the performance of the cognitive relaying networks was examined in [54] using multiple antenna-receivers and DF multihop relaying.

For composite fading channels, the outage probability of CR was analyzed for SU systems with relays in [55] over independent and identical distribution (i.i.d) generalized-K composite fading channels only for the peak power constraint. For multipath fading, the outage and ergodic capacities increase rapidly when the fading parameter decreases. For the multihop spectrum-sharing relaying, the ergodic capacity and the BER were studied in the composite fading channels. The analysis was done under the peak power constraint where the upper-bound and lower-bound expressions were derived for the ergodic capacity and the average BER, respectively [56]. Fur-

thermore, dual-hop relays were used in [57] to analyze the ergodic capacity of CR network over non-identical generalized-K composite fading channels.

CHAPTER 3

CAPACITY OF CR WITH SINGLE PU

3.1 Introduction

Chapter three contains a thorough performance analysis for an underlay CR network capacity with a single PU over generalized-K composite fading channels. In addition, the performance metrics, ergodic capacity and outage probability, are analyzed by taking the consideration of peak and average power constraints. Moreover, for both performance metrics, closed-form expressions are derived in terms of special functions that can be computed using Matlab or Mathematica software. Up to our best knowledge, no work in open literature has investigated the CR capacity for the average received-power constraint over generalized-K composite fading channels. Furthermore, the remainder of this chapter is arranged as follows: Section

3.2 describes both the system and channel models; Sections 3.3, and 3.4 provide the analysis for ergodic capacity and outage probability, respectively; Section 3.5 discusses the results and simulations; and Section 3.6 states the conclusions.

3.2 System Model-Single PU

As illustrated in Fig. 3.1, the system model for the underlay CR network involves non-cognitive receiver (PU-Rx), a cognitive receiver (SU-Rx), and a cognitive transmitter (SU-Tx). In addition, the PU has the right to utilize the spectrum band freely. On the other hand, the SU is permitted to share the frequency band without harming the PU. So, in this model, the SU

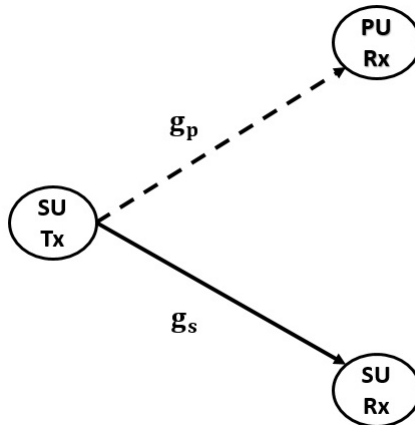


Figure 3.1: System model - Single PU.

operates on the PU's band when the received power at the PU-Rx does not exceed a specific interference threshold Q . The g_s and g_p indicate the instantaneous channel gains for both links SU-Tx to PU-Rx and SU-Tx to

SU-Rx, respectively. Both channel gains are supposed to be ergodic and stationary with flat fading and perfect CSI. The g_s and g_p are assumed to model the joint effect of multipath fading as well as shadowing.

Composite fading is usually modeled using Log-normal-based models; however, the generalized-K composite fading model has lately received interest as a more tractable model that has allowed obtaining closed-form expressions for several performance metrics (refer to [16] and the references therein). The PDF of the generalized-K model is given as in (2.9).

3.3 Ergodic Capacity

3.3.1 Ergodic Capacity Under Average Received-Power Constraint

In this section, the closed-form expressions of the SU ergodic capacity over generalized-K composite channel are derived. The channel capacity in the fading environment is achieved by finding the optimal power allocation. For this reason, the next optimization problem should be solved to obtain the channel capacity [36],

$$\begin{aligned}
 C &= \max_{P(g_p, g_s) \geq 0} E \left[B \log \left(1 + \frac{g_s P(g_p, g_s)}{N_0 B} \right) \right], \\
 \text{s.t. } & E [g_p P(g_p, g_s)] \leq Q_{av}
 \end{aligned} \tag{3.1}$$

Then (3.1) can be rewritten as,

$$C = \max_{P(g_p, g_s) \geq 0} \int_{g_p} \int_{g_s} B \log \left(1 + \frac{g_s P(g_p, g_s)}{N_o B} \right) f_p(g_p) f_s(g_s) dg_p dg_s, \quad (3.2)$$

$$\text{s.t.} \quad \int_{g_p} \int_{g_s} g_p P(g_p, g_s) f_p(g_p) f_s(g_s) dg_p dg_s \leq Q_{av},$$

where Q_{av} is the maximum average power tolerated at the PU-Rx, $P(g_p, g_s)$ is the optimal power allocation. By using the Lagrangian method to obtain the optimal power allocation from (3.1), the $P(g_p, g_s)$ can be obtained as,

$$P(g_p, g_s) = \left(\frac{1}{\lambda_o g_p} - \frac{N_o B}{g_s} \right)^+, \quad (3.3)$$

where $(\cdot)^+$ is $\max(\cdot, 0)$, λ_o indicates the Lagrange multiplier used to find the optimal power allocation and it can be found from (3.1) when the average received-power constraint equals to Q_{av} . From (3.3), it can be seen that the cutoff level for g_s is obtained when $g_s = \lambda_o N_o B g_p$. Moreover, if $\frac{g_s}{g_p}$ is greater than $\lambda_o N_o B$, the data will be transmitted. More importantly, the ergodic capacity over fading channels was derived in [38] with assuming full CSI at the receiver and the transmitter, respectively as,

$$C = B \int_{\frac{1}{\gamma_0}}^{\infty} \log(\gamma_0 \chi) f_{\frac{g_s}{g_p}}(\chi) d\chi, \quad (3.4)$$

where the random variable (RV) $\chi = \frac{g_s}{g_p}$, $f_{\frac{g_s}{g_p}}(\cdot)$ is the PDF of χ , $\alpha = \frac{Q_{av}}{N_o B}$, $\gamma_0 = \frac{1}{\lambda_o N_o B}$. The parameter γ_0 is obtained by solving the following equation

for a given α ,

$$\alpha = \int_0^{\gamma_0} (\gamma_0 - \chi) f_{\frac{g_s}{g_p}}(\chi) d\chi, \quad (3.5)$$

For the generalized-K composite fading model, we have the parameters m_{mp} , m_{ms} , m_{sp} , and m_{ss} for the power gains g_p and g_s . For the PU signal, the parameters m_{mp} and m_{sp} characterize fading and shadowing, respectively. Similarly, For the SU signal, m_{ms} and m_{ss} characterize multipath fading and shadowing.

In this respect, the PDF of χ for generalized-K composite fading channels, where both g_p and g_s are independent RVs, is given by [16],

$$f_{\frac{g_s}{g_p}}(\chi) = \Psi G_{2,2}^{2,2} \left(\Delta \chi \left| \begin{matrix} -m_{mp}, -m_{sp} \\ m_{ms} - 1, m_{ss} - 1 \end{matrix} \right. \right), \chi > 0, \quad (3.6)$$

where $\Psi = \frac{m_{ms}m_{ss}\Omega_{0,p}}{\Gamma(m_{ms})\Gamma(m_{ss})\Gamma(m_{mp})\Gamma(m_{sp})m_{mp}m_{sp}\Omega_{0,s}}$, $\Delta = \left(\frac{m_{ms}m_{ss}\Omega_{0,p}}{m_{mp}m_{sp}\Omega_{0,s}} \right)$, and $G_{p,q}^{m,n} \left(\chi \left| \begin{matrix} a_p \\ b_q \end{matrix} \right. \right)$ represents the Meijer G-function [24, (9.301)]. By substituting (3.6) in (3.5), the α can be obtained by using [58, (2.24.2.2)] as,

$$\int_0^{\gamma_0} (\gamma_0 - \chi) \times \Psi G_{2,2}^{2,2} \left(\Delta \chi \left| \begin{matrix} -m_{m,p}, -m_{s,p} \\ m_{m,s} - 1, m_{s,s} - 1 \end{matrix} \right. \right) d\chi = \alpha,$$

$$\alpha \Psi^{-1} = G_{3,3}^{2,3} \left(\Delta \gamma_0 \left| \begin{matrix} -m_{mp} + 2, -m_{sp} + 2, 2 \\ m_{ms} + 1, m_{ss} + 1, 1 \end{matrix} \right. \right) - G_{3,3}^{2,3} \left(\Delta \gamma_0 \left| \begin{matrix} -m_{mp} + 2, -m_{sp} + 2, 1 \\ m_{ms} + 1, m_{ss} + 1, 0 \end{matrix} \right. \right). \quad (3.7)$$

By inserting (3.5) in (3.4) and performing the integration numerically, the ergodic capacity can be obtained.

Remark I: For large γ_0 , the ergodic capacity can be obtained by utilizing the Meijer G-function in terms of the logarithm function [58, (8.4.6.5)], $\log(\gamma_0 \chi) = G_{2,2}^{1,2} \left(\gamma_0 (\chi - 1) \left| \begin{matrix} 1, 1 \\ 1, 0 \end{matrix} \right. \right)$. Afterwards, by using the integration formula in [24, (7.811.1)], the ergodic capacity can be approximated as,

$$C \approx B \int_0^\infty G_{2,2}^{1,2} \left(\gamma_0 (\chi - 1) \left| \begin{matrix} 1, 1 \\ 1, 0 \end{matrix} \right. \right) \times \Psi G_{2,2}^{2,2} \left(\Delta \chi \left| \begin{matrix} -m_{mp}, -m_{sp} \\ m_{ms} - 1, m_{ss} - 1 \end{matrix} \right. \right) d\chi,$$

$$C \approx \frac{B \Psi}{\Delta} G_{4,4}^{3,4} \left(\frac{\gamma_0}{\Delta} \left| \begin{matrix} -(m_{ms} - 1), -(m_{ss} - 1), 1, 1 \\ m_{mp}, m_{sp}, 1, 0 \end{matrix} \right. \right) \quad (3.8)$$

Also, this expression can be utilized for the exact ergodic capacity for the peak received power constraint in the i.n.d generalized-K composite fading channels.

However, closed-form expressions for both the parameter α and the ergodic capacity can be derived for the following interesting cases (see Appendix A.1).

Case I: Rayleigh multipath fading channels with heavy shadowing ($m_m = 1$ and $m_s = 0.5$).

In this case, for the equivalent Log-normal shadowing model, the corresponding dB-spread (σ_s) is 9.1 dB. For this case, the PDF can be derived as,

$$f_{\frac{g_s}{g_p}}(\chi) = \frac{1}{2\sqrt{\chi}(\sqrt{\chi} + 1)^2}, \quad \chi \geq 0. \quad (3.9)$$

Moreover, the expressions for both α parameter and ergodic capacity are obtained as,

$$\gamma_0 + 2 \log(1 + \sqrt{\gamma_0}) - 2 \sqrt{\gamma_0} = \alpha, \quad (3.10)$$

and,

$$C = B \left[\log(\gamma_0) + 2 \log\left(1 + \frac{1}{\gamma_0}\right) \right]. \quad (3.11)$$

The obtained theoretical PDF expression is verified by Monte Carlo simulations as shown in Fig. 5.2.

Case II: Rayleigh multipath fading with moderate shadowing
($m_m = 1$ and $m_s = 2$).

In addition, the dB-spread (σ_s) is 5.5 dB. The PDF of Rayleigh multipath fading with moderate shadowing can be derived as,

$$f_{\frac{g_s}{g_p}}(\chi) = \frac{\chi^3 + 9\chi^2 - 3\chi(3 + 2(1 + \chi)\log(\chi)) - 1}{0.5(\chi - 1)^5}, \quad (3.12)$$

Furthermore, the ergodic capacity and the parameter α may be derived as,

$$\alpha = \frac{\gamma_0^2(\gamma_0^2 - 2\gamma_0\log(\gamma_0) - 1)}{(\gamma_0 - 1)^3}. \quad (3.13)$$

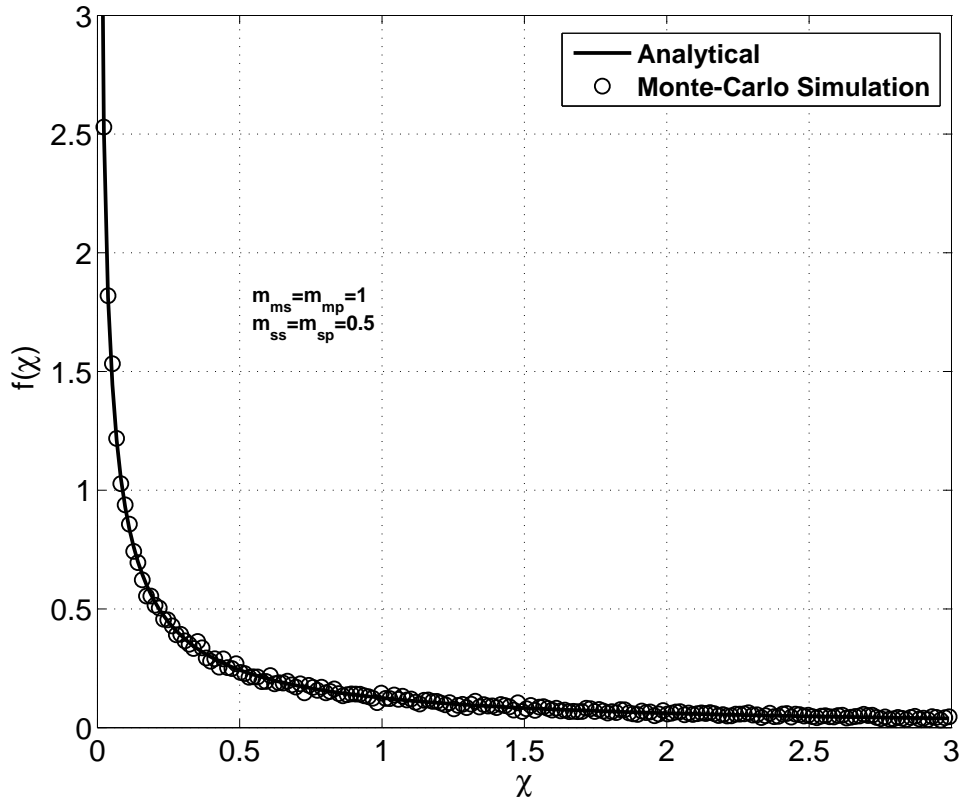


Figure 3.2: The Monte-Carlo simulation and analytical plots for the $f(\chi)$ of Rayleigh multipath fading channels with heavy shadowing

and,

$$C = B \left[\log(\gamma_0) + \frac{\log(\gamma_0)(1 - 3\gamma_0) + 2\gamma_0(\gamma_0 - 1)}{(\gamma_0 - 1)^3} \right]. \quad (3.14)$$

Again, the complete match between the analytical PDF expression and the Monte-Carlo simulation is shown in Fig. 3.3.

Remark II: In both (3.11) and (3.14), we note that there are additional terms due to the effect of the shadowing as compared to the capacity of unshadowed Rayleigh as in (3.17). Moreover, from the capacity expressions of both cases, we may observe that the additional terms in (3.11) and (3.14)

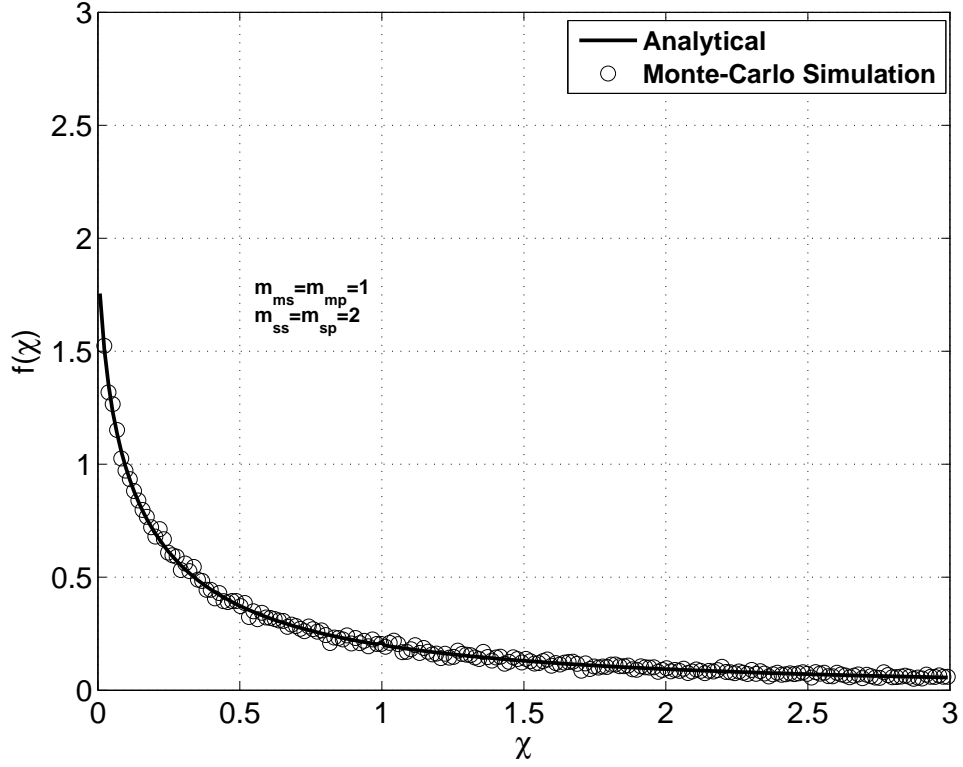


Figure 3.3: The Monte-Carlo simulation and analytical plots for the $f(\chi)$ of Rayleigh multipath fading with moderate shadowing.

will vanish for large γ_0 to reduce the ergodic capacity expression to $\log(\gamma_0)$ for both shadowed and unshadowed Rayleigh channels as demonstrated in the numerical results part.

For the unshadowed Rayleigh channel ($m_m = 1$), the channel gains g_p , and g_s have exponential distribution with unit mean. As a result, the RV $\frac{g_s}{g_p}$ has a simpler distribution which is the log-logistic distribution as,

$$f_{\frac{g_s}{g_p}}(\chi) = \frac{1}{(1 + \chi)^2}, \quad \chi \geq 0, \quad (3.15)$$

By substituting (3.15) in (3.5), the parameter α is obtained as in [38] as,

$$\gamma_0 - \log(1 + \gamma_0) = \alpha \quad (3.16)$$

and

$$C = B \log(1 + \gamma_0) \quad (3.17)$$

3.3.2 Ergodic Capacity over Nakagami Fading Channel

This section investigates and analyzes the ergodic capacity of the CR networks over Nakagami fading channels. For the average power constraint, closed-form expressions are derived. The ratio PDF of $\frac{g_s}{g_p}$ is given by [59],

$$f_{\frac{g_s}{g_p}}(\chi) = \left(\frac{m_{mp}}{m_{ms}}\right)^{m_{mp}} \frac{x^{m_{ms}-1}}{\beta(m_{mp}, m_{ms}) \left(\chi + \frac{m_{mp}}{m_{ms}}\right)^{m_{mp}+m_{ms}}}, \quad \chi \geq 0, \quad (3.18)$$

where $\beta(m_{mp}, m_{ms})$ denotes the beta function that can be represented as,

$$\beta(m_{mp}, m_{ms}) = \frac{\Gamma(m_{mp})\Gamma(m_{ms})}{\Gamma(m_{mp}+m_{ms})}. \quad \text{When } m_m = m_{mp} = m_{ms}, \quad (3.18) \text{ can be}$$

reduced to,

$$f_{\frac{g_s}{g_p}}(\chi) = \frac{x^{m_m-1}}{\beta(m_m, m_m) (\chi + 1)^{2m_m}}, \quad \chi \geq 0, \quad (3.19)$$

By substituting (3.19) in (3.5), the parameter α can be obtained as,

$$\alpha = \frac{\gamma_0^{m_m+1} {}_2F_1(m_m, 2m_m; m_m + 1; -\gamma_0)}{m_m \beta(m_m, m_m)} - \frac{\gamma_0^{m_m+1} {}_2F_1(2m_m, m_m + 1; m_m + 2; -\gamma_0)}{(m_m + 1) \beta(m_m, m_m)}. \quad (3.20)$$

By substituting (3.19) in (3.4), the ergodic capacity can be obtained as,

$$C = \frac{B (\gamma_0^{m_m}) \times \{ {}_3F_2(m_m, m_m, 2m_m; 1 + m_m, 1 + m_m; -\gamma_0) \}}{\beta(m_m, m_m) m_m^2}. \quad (3.21)$$

The detailed derivation is given in Appendix A.1.

3.3.3 Ergodic Capacity Under Peak Received-Power Constraint

This section considers the ergodic capacity of the SU for peak received-power constraint where closed-form expressions are derived. However, the type of the power constraint depends on the QoS used by the PU. Hence, if the instantaneous QoS is provided by the PU, the peak received-power constraint is used. Let Q_{peak} represent the peak received power at PU-Rx [39] and it can be expressed as,

$$g_p P(g_p, g_s) \leq Q_{peak} \quad (3.22)$$

From (3.22), it can be seen that the maximum instantaneous power permitted by PU-Rx is $\frac{Q_{peak}}{g_p}$. Therefore, the ergodic capacity can be obtained by

substituting (3.22) in (3.2) as,

$$C = B \int_0^\infty \log(1 + \alpha\chi) f_{\frac{g_s}{g_p}}(\chi) d\chi \quad (3.23)$$

where the parameter $\alpha = \frac{Q_{peak}}{N_o B}$. The ergodic capacity of the SU can be derived by substituting (3.6) in (3.23). Hence, the ergodic capacity is evaluated as,

$$C = \int_0^\infty B \log(1 + \alpha\chi) \times \Psi G_{2,2}^{2,2} \left(\Delta \chi \left| \begin{matrix} -m_{mp}, -m_{sp} \\ m_{ms} - 1, m_{ss} - 1 \end{matrix} \right. \right) d\chi \quad (3.24)$$

By using the representation of the logarithm function in terms of the Meijer G-function [58, (8.4.6.5)], $\log(1 + \alpha\chi) = G_{2,2}^{1,2} \left(\alpha\chi \left| \begin{matrix} 1, 1 \\ 1, 0 \end{matrix} \right. \right)$, the integration in (3.24) can be written as,

$$C = B \int_0^\infty G_{2,2}^{1,2} \left(\alpha\chi \left| \begin{matrix} 1, 1 \\ 1, 0 \end{matrix} \right. \right) \times \Psi G_{2,2}^{2,2} \left(\Delta \chi \left| \begin{matrix} -m_{mp}, -m_{sp} \\ m_{ms} - 1, m_{ss} - 1 \end{matrix} \right. \right) d\chi \quad (3.25)$$

Then, by using the integration formula in [24, (7.811.1)], the ergodic capacity can be obtained as,

$$C = \frac{B \Psi}{\Delta} G_{4,4}^{3,4} \left(\frac{\alpha}{\Delta} \left| \begin{matrix} -(m_{ms} - 1), -(m_{ss} - 1), 1, 1 \\ m_{mp}, m_{sp}, 1, 0 \end{matrix} \right. \right) \quad (3.26)$$

Nevertheless, the ergodic capacity expressions can be simplified to the next practical cases:

Case I: Rayleigh multipath fading channels with heavy shadowing.

By substituting the PDF (3.9) in (3.23) and evaluating the integral, the ergodic capacity is expressed as,

$$C = B \left[\frac{\pi\sqrt{\alpha} + \alpha \log(\alpha)}{1 + \alpha} \right] \quad (3.27)$$

Case I: Rayleigh multipath fading channels with moderate shadowing.

By substituting the PDF (3.12) in (3.23) and evaluating the integral, the ergodic capacity is derived as,

$$C = B\alpha \left[\frac{(1 + \alpha)(-2 + \alpha(5 + \alpha)) \log(\alpha) + 3\alpha \log(\alpha)^2 - 3(1 + \alpha)[2 - \pi^2 + \alpha]}{(1 + \alpha)^2} \right] \quad (3.28)$$

3.4 Outage Probability

3.4.1 Outage Probability Under Average-Power Constraints

This section presents the outage probability (P_{out}) of CR networks over generalized-K composite fading channels where closed-form expressions are derived while taking into consideration the average power constraint. The

optimization problem can be described as [39],

$$\min_{P(g_p, g_s)} P_{out} \left\{ \log_2 \left(1 + \frac{g_s P(g_p, g_s)}{N_0} \right) < R \right\}, \quad (3.29)$$

$$s.t. \ E [g_p P(g_p, g_s)] \leq Q_{av},$$

The P_{out} for a given target rate R , $P_{out}(R)$, over fading channels assuming perfect CSI at SU-Tx was derived in [39] as,

$$P_{out} = 1 - P \left\{ \frac{g_s}{g_p} < y \right\} = 1 - \int_0^y f_{\frac{g_s}{g_p}}(\chi) d\chi, \quad (3.30)$$

where $y = \frac{1}{\lambda_0 N_0 (2^R - 1)}$ is obtained by solving (3.31) for a given Q_{av} ,

$$\int_0^y \chi f_{\frac{g_s}{g_p}}(\chi) d\chi = \frac{Q_{av}}{N_0 (2^R - 1)}, \quad (3.31)$$

Then, the closed-form expression for the outage probability can be derived by substituting (3.6) in (3.30) and evaluating the integration to get,

$$P_{out}(R) = 1 - \Psi y G_{3,3}^{2,3} \left(\Delta y \left| \begin{array}{c} -m_{mp}, -m_{sp}, 0 \\ m_{ms} - 1, m_{ss} - 1, -1 \end{array} \right. \right) \quad (3.32)$$

Also, by substituting (3.6) in (3.31), we get,

$$\Psi y^2 G_{3,3}^{2,3} \left(\Delta y \left| \begin{array}{c} -m_{mp}, -m_{sp}, -1 \\ m_{ms} - 1, m_{ss} - 1, -2 \end{array} \right. \right) = \frac{Q_{av}}{N_0 (2^R - 1)}, \quad (3.33)$$

Moreover, the closed-form expressions for both the Q_{av} and the outage probability simplifies for the following interesting cases as shown in Appendix B.

Case I: Rayleigh multipath fading with heavy shadowing channel.

For this case, the expressions for both Q_{av} and outage probability can be simplified as,

$$P_{out}(R) = \frac{1}{1 + \sqrt{y}}. \quad (3.34)$$

and,

$$\frac{\sqrt{y} (2 + \sqrt{y})}{1 + \sqrt{y}} - 2\log(1 + \sqrt{y}) = \frac{Q_{av}}{N_o (2^R - 1)}, \quad (3.35)$$

Case II: Rayleigh multipath fading with moderate shadowing channel.

The expressions for both Q_{av} and outage probability can be simplified as,

$$P_{out}(R) = \frac{2y^3 + 3y^2 (1 - 2\log(y)) - 6y + 1}{(y - 1)^4}. \quad (3.36)$$

and,

$$\frac{y^2(1 + (4 - 5y)y + 2y(2 + y)\log(y))}{(y - 1)^4} = \frac{Q_{av}}{N_o (2^R - 1)}. \quad (3.37)$$

For the unshadowed Rayleigh channel ($m_m = 1$), By substituting (3.15) in (3.30), the outage probability is obtained in [39] as,

$$P_{out} = \frac{1}{1 + y}. \quad (3.38)$$

where y is obtained as,

$$\log(1 + y) - \frac{y}{1 + y} = \frac{Q_{av}}{N_o(2^R - 1)}, \quad (3.39)$$

Remark III: The outage probability expression in (3.34) results in higher outage probability as compared to unshadowed Rayleigh channel in (3.38) for high SNR as shown in the result and simulation part.

3.4.2 Outage Probability Under Peak Received-Power Constraint

The outage probability can be derived for generalized-K composite fading channels for the peak received-power constraint in (3.22) as,

$$P_{out}(R) = \int_0^z f_{\frac{g_s}{g_p}}(\chi) d\chi, \quad (3.40)$$

where $z = \frac{N_o(2^R - 1)}{Q_{peak}}$. By substituting (3.6) in (3.40), we get,

$$P_{out}(R) = \Psi z G_{3,3}^{2,3} \left(\Delta z \left| \begin{array}{c} -m_{mp}, -m_{sp}, 0 \\ m_{ms} - 1, m_{ss} - 1, -1 \end{array} \right. \right) \quad (3.41)$$

and can be simplified to the following cases:

Case I: For Rayleigh multipath fading with heavy shadowing channels, the

$P_{out}(R)$ can be reduced to,

$$P_{out}(R) = \frac{\sqrt{z}}{1 + \sqrt{z}} \quad (3.42)$$

$$P_{out}(R) = \frac{\sqrt{N_0(2^R - 1)}}{\sqrt{Q_{peak}} + \sqrt{N_0(2^R - 1)}} \quad (3.43)$$

Case II: For Rayleigh multipath fading with moderate shadowing channels, the $P_{out}(R)$ expressions can be reduced to,

$$P_{out}(R) = \frac{z(6z \log(z) + z(3 + z(z - 6)) + 2)}{(z - 1)^4} \quad (3.44)$$

3.5 Results and Discussions

In this section of the thesis work, some simulations and analytical results of the discussed topics are presented and investigated.

3.5.1 Ergodic Capacity

In Fig. 3.4, the ergodic capacity of the SU is depicted for Nakagami fading and AWGN cases with average power constraint. For $m = 1$, the capacity of the SU is larger than the other cases for all values of Q_{av} . The capacity of the SU increases as a result of the effect of the multipath fading. As a result, the SU takes the advantage of this situation by transmitting a higher

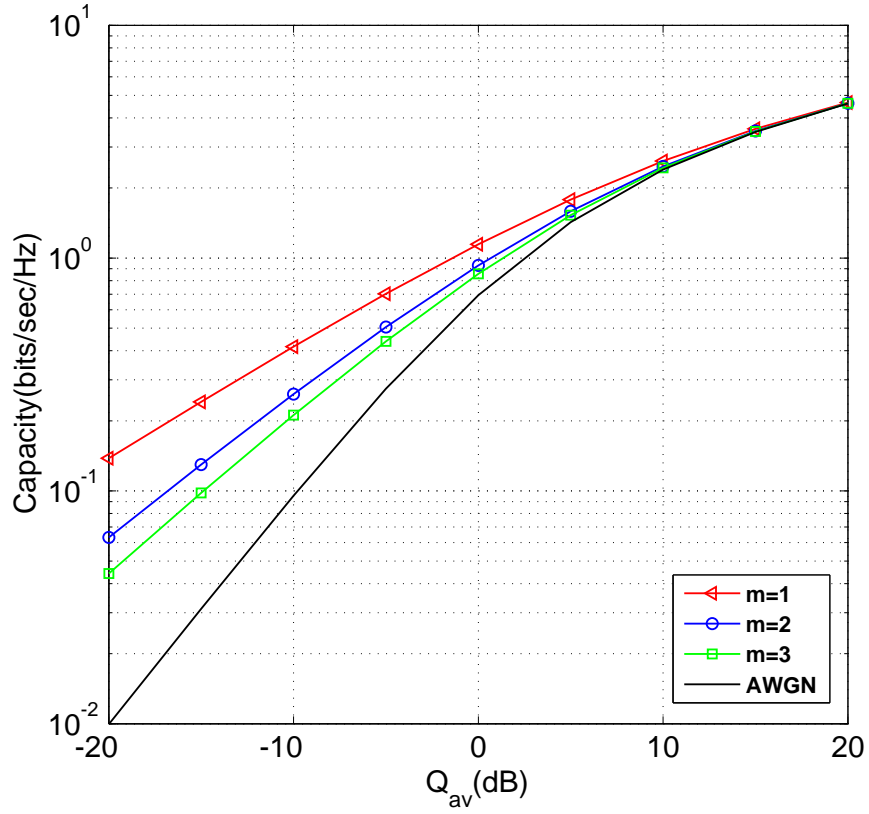


Figure 3.4: The ergodic capacity of the SU for several Nakagami fading scenarios.

power without harming the PU-Rx.

The capacity of the SU over generalized-K fading channels is shown in Fig. 3.5 under the average received-power constraint. Three cases are considered: Rayleigh multipath fading with heavy shadowing, Rayleigh multipath fading with moderate shadowing, and unshadowed Rayleigh channels. In addition, the results are compared to the AWGN case.

Another interesting point is that the ergodic capacity of the SU gets higher as m_m , the multipath parameter, and m_s , the shadowing parameter, get smaller. In the Rayleigh multipath fading with heavy shadowing channels

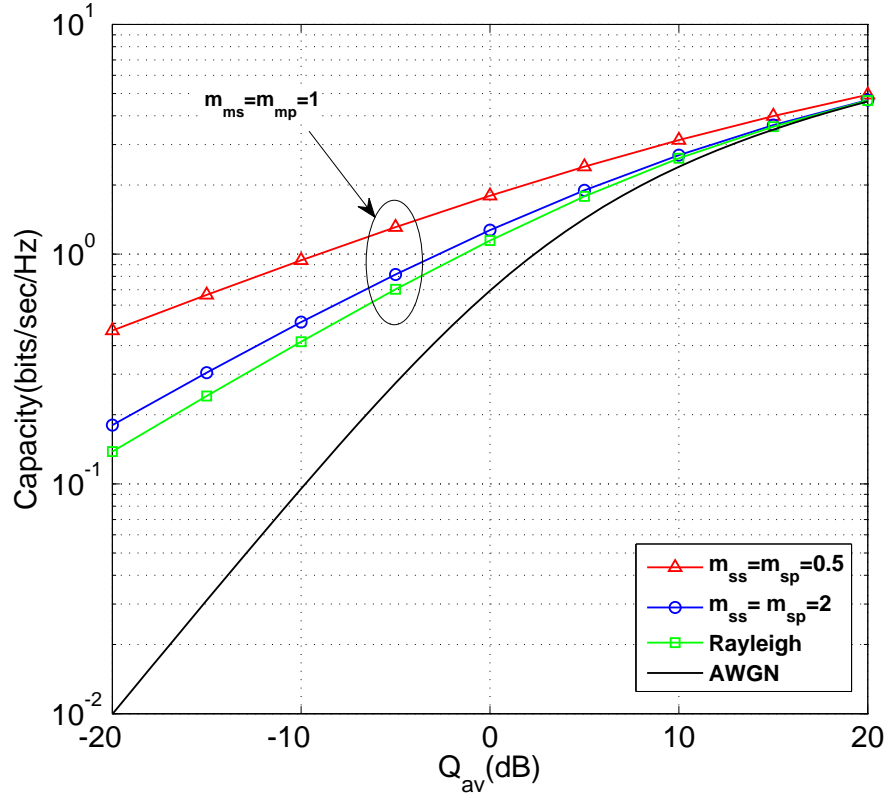


Figure 3.5: Ergodic capacity of SU for different composite fading scenarios.

($m_m = 1$ and $m_s = 0.5$) the SU has the maximum capacity at low Q_{av} . For the Rayleigh multipath fading with moderate shadowing channels ($m_m = 1$ and $m_s = 2$) the capacity of SU is close to the case of unshadowed Rayleigh channel. Another interesting point is that for all the cases, the capacity of SU approaches AWGN at high Q_{av} as the effect of fading diminishes.

However, Fig. 3.6 represents the ergodic capacity of SU for both the peak and average power constraints ($Q_{peak} = Q_{av} = Q$), respectively for Rayleigh multipath fading with heavy shadowing, Rayleigh multipath fading with moderate shadowing. It can be observed that the capacity of the SU increases the shadowing parameter m_s gets smaller. It can also be seen that

the capacity of SU for the Q_{peak} is higher than the Q_{av} case as a consequence of that the peak power constraint is more restrictive than the average power constraint. For all cases, the capacity of SU approaches AWGN at high Q_{peak} and Q_{peak} as the effect of fading diminishes as expected.

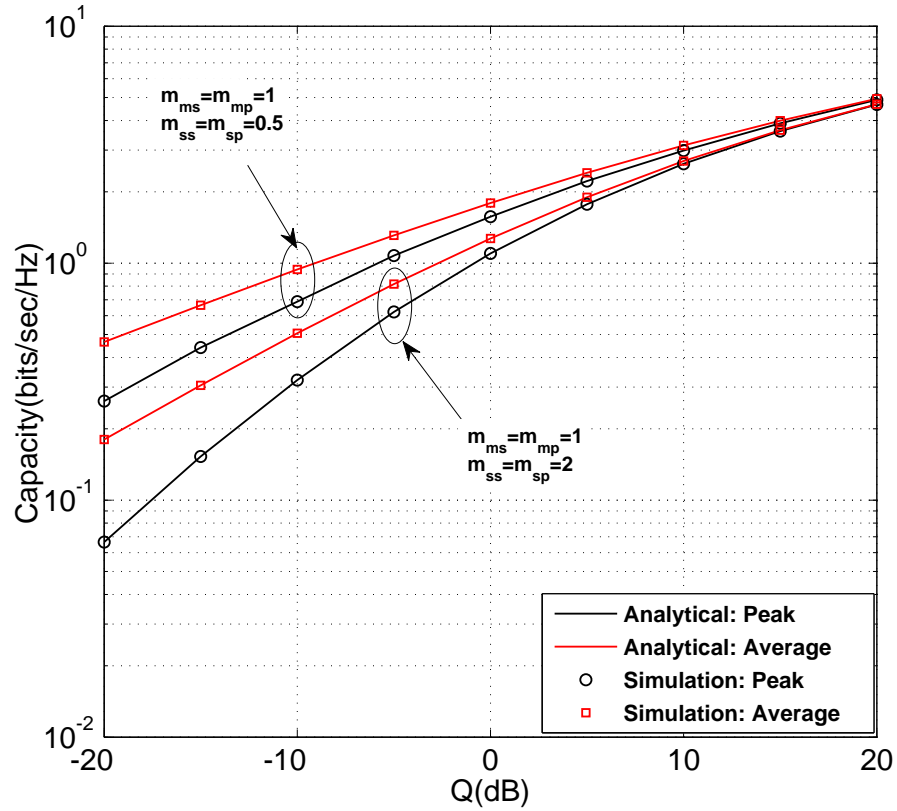


Figure 3.6: Ergodic capacity of SU for different composite fading scenarios for $Q_{av} = Q_{peak} = Q$.

For i.n.d. case with peak power constrains, the ergodic capacity is illustrated in Fig. 3.7. We can note that the role of the m_{sp} parameter (i.e, the shadowing conditions of the PU link) is the dominant one where the maximum capacity is obtained when the PU link is in heavy shadowing.

The generalized-K distribution can be approximated by using single Gamma

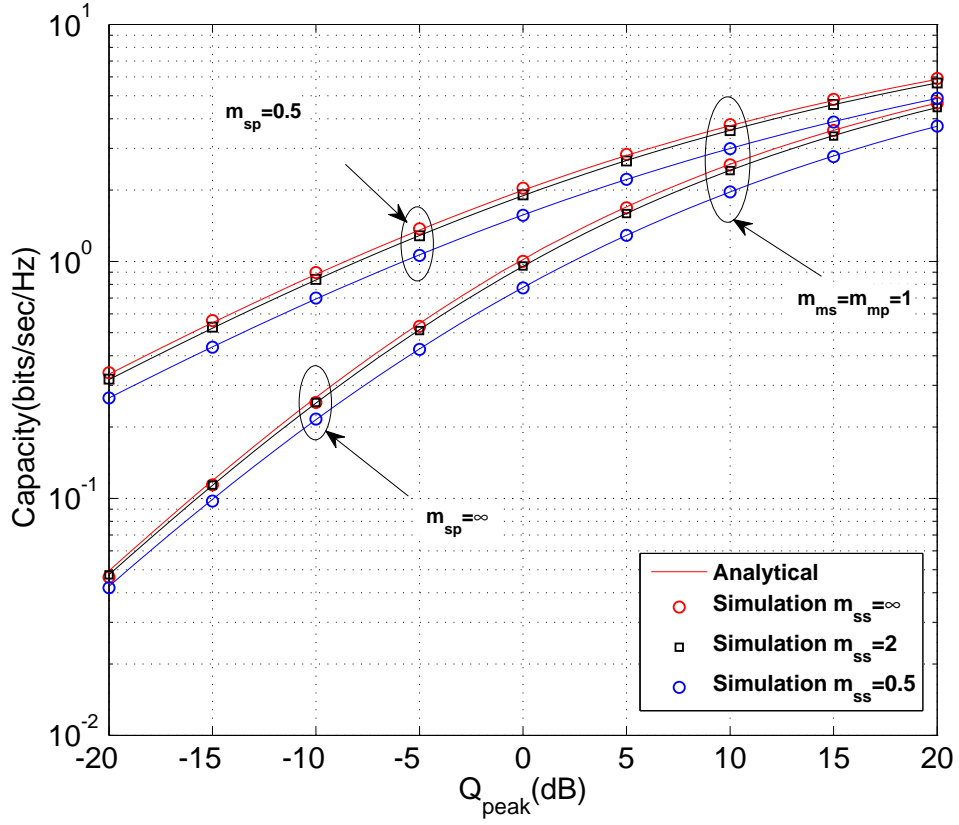


Figure 3.7: Ergodic capacity of SU for different composite fading scenarios.

distribution where the parameters are obtained by using (2.10). In Fig. 3.8, the comparison between the exact and the approximation for the generalized-K composite fading channel is illustrated for different values of multipath and shadowing parameters. In addition, different ϵ values are used. For the first case, $K(1,0.5,1) \approx G(0.38,2.6)$, the exact and the approximation curves match very well in high Q_{av} while there is a difference at low Q_{av} . The similar observation appears for the other two cases.

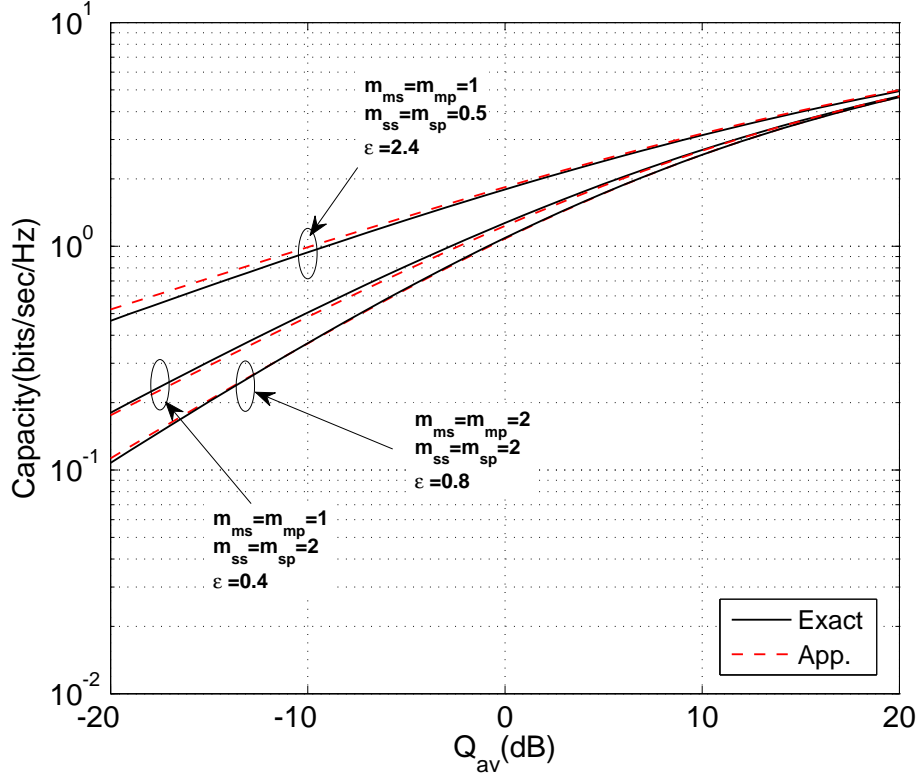


Figure 3.8: Ergodic capacity for both exact and approximation cases.

3.5.2 Outage Probability

Figure 3.9, illustrates the outage probability of the SU vs Q_{av} for the generalized-K composite fading channel. The target rate is $R = 1$ bit/sec/Hz. Moreover, the outage probability is shown for three scenarios: Rayleigh multipath fading with heavy shadowing, Rayleigh multipath fading with moderate shadowing, and unshadowed Rayleigh multipath fading channels. Furthermore, for small Q_{av} , the curves overlap for all the scenarios. The major effect of heavy shadowing on the outage probability is demonstrated in Fig. 3.9 where the probability of outage at 5 dB for heavy shadowing is 0.15 and it decreases to 0.04 and 0.17 for moderate shadowing

and unshadowed Rayleigh, respectively. At small Q_{av} , below the overlap point, the effect of m_{sp} is dominant as compared to m_{ss} . On the other hand, m_{ss} is dominant for large Q_{av} . Then, the Rayleigh with heavy shadowing is better than the others.

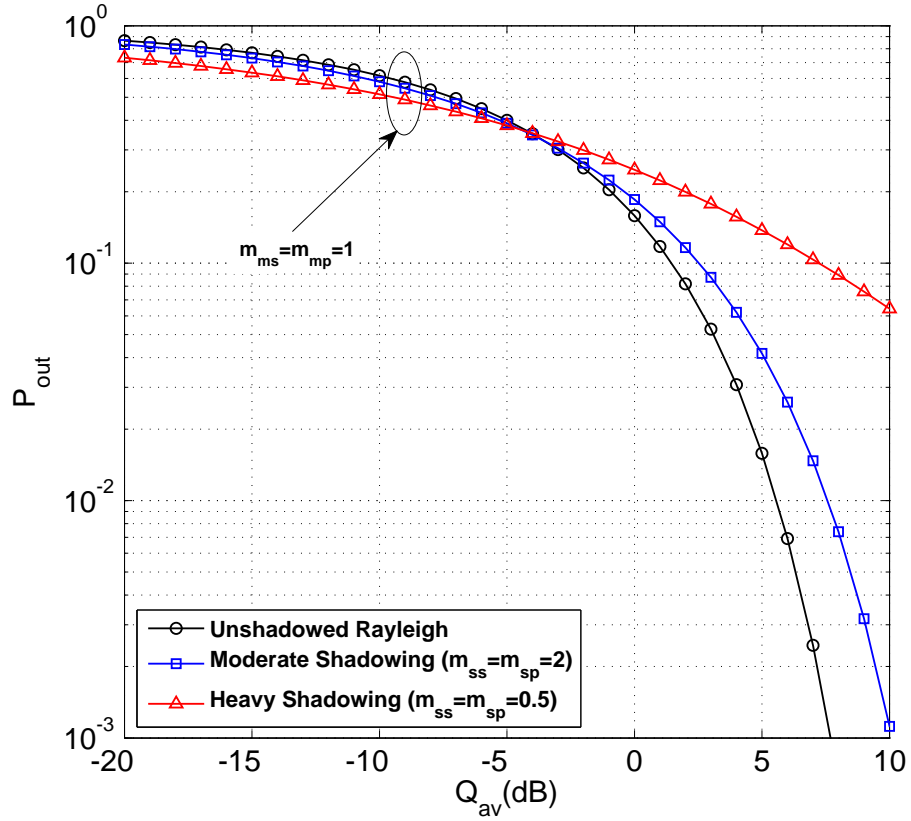


Figure 3.9: Outage probability of generalized-K Composite fading channel for Q_{av} .

The effect of the SU shadowing m_{ss} parameter is dominant as compared to the m_{sp} parameter as shown in Fig. 3.10.

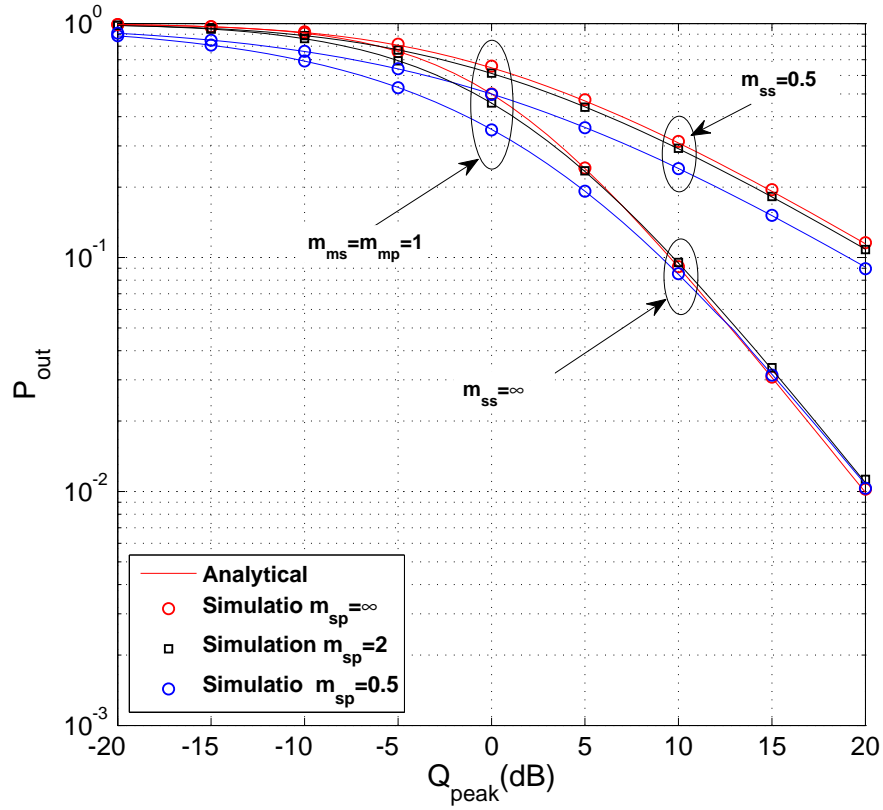


Figure 3.10: Outage probability of SU for different composite fading scenarios.

3.6 Conclusions

In this chapter, we considered both the ergodic capacity and outage probability of underlay CR networks over generalized-K composite fading channels under both average and peak received-power constraints. For the ergodic capacity and the outage probability under both the average and peak power constraints, closed-form expressions are derived. To gain more insights, two tractable relevant composite fading scenarios: Rayleigh multipath fading with heavy shadowing and Rayleigh multipath fading with moderate shadowing for single PU are studied in details. The obtained results quantified

the increase in the ergodic capacity and the decrease of the outage probability for the SU because of the joint effect of both multipath fading and shadowing for single PU. In addition, the results show that the peak constraints are more restrictive than average constraints. As a result, from CR networks perspective, the average power constraints are better from peak constraints because of gaining more capacity. However, the obtained results will serve as a benchmark for other architectures of underlay CR networks.

CHAPTER 4

CAPACITY ANALYSIS OF CR WITH MULTIPLE PRIMARY USERS

4.1 Introduction

In this chapter, the analysis of CR network capacity with multiple PUs is provided over generalized-K composite fading channels. The ergodic capacity and outage probability of underlay CR are studied under the peak received-power constraint. In our analysis, we derive closed-form expressions for the ergodic capacity and the outage probability for two interesting cases: Rayleigh multipath fading with heavy and moderate shadowing.

The ergodic capacity of underlay CR networks with multiple PUs was consid-

ered in [38] for only the Rayleigh multipath fading model. Both the ergodic capacity and outage probability are analyzed under peak constraint of multiple PUs over Nakagami fading channels for single-relay CR networks in [60]. Moreover, the derivations were extended to the effect of interference caused by the PU transmitters on the SU relay and SU receiver in [61]. The best relay selection scheme was considered in [62] to analyze the outage capacity over Nakagami multipath fading channels where closed-form expression was derived. In addition, the analysis was extended for imperfect CSI in [63]. For CR with multihop relaying, the outage probability and ergodic capacity were studied in [64] for multiple PUs over Nakagami multipath fading channel. In [65], the orthogonal spectrum band is utilized to minimize the interference caused by SU transmitter and SU relays on the PUs.

To the best of our knowledge, no work in open literature has investigated the CR capacity with multiple PUs for the peak received-power constraint over shadowed multipath fading channels. So, the purpose of this chapter is to analyze the performance metrics of CR networks for peak power constraint over shadowed Rayleigh composite fading channels. The remainder of this chapter is arranged as the following; Section 4.2, outlines both the system and channel models; Section 4.3 provides the performance; Section 4.4 discusses the obtained results; and Section 4.5 states the conclusion.

4.2 System and Channel Models

Considering an underlay CR network with multiple PUs, the system model for the underlay CR comprises multiples non-cognitive receivers (PU-Rxj), SU-Tx, and SU-Rx as illustrated in Fig. 4.1. In this model, the SU operates on the PU's band when the received power at the PU-Rxs does not exceed a specific interference threshold Q_{peak} . The ergodic and stationary g_s and g_{pj} are assumed to model the joint effect of shadowing as well as multipath fading.

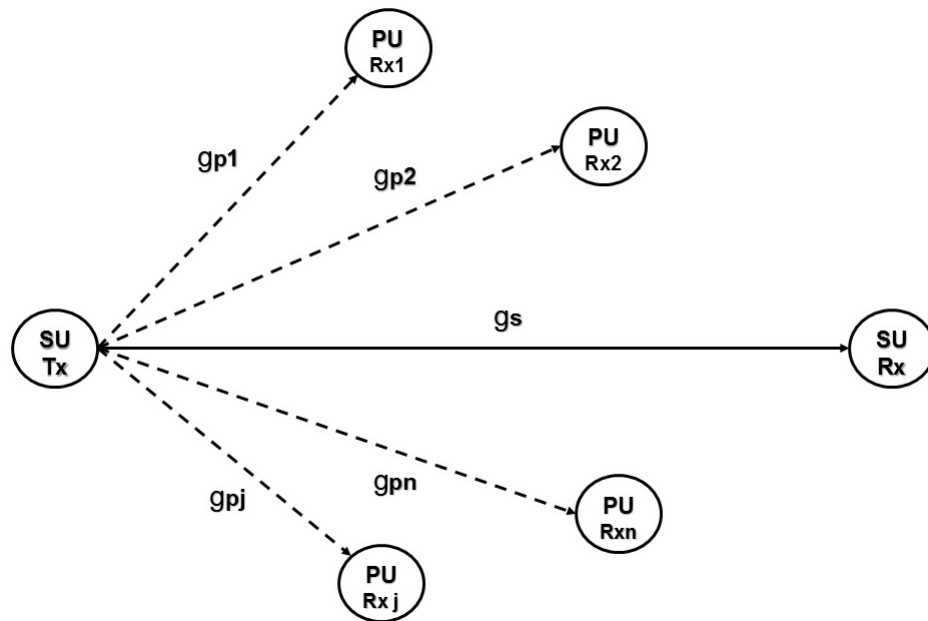


Figure 4.1: System model- multiple PUs.

4.3 Capacity of CR Network with Multiple Primary Users

In this section, closed-form expressions of the capacity are derived for some tractable interesting scenarios of multipath fading shadowing scenarios for the peak power constraint as general expressions for any value of m_m and m_s are not tractable. The analysis is performed to multiple PUs with single SU. For this model, the transmitted power of the SU is undergone to more power constraints. As a result, the CR capacity decreases. In this model, the capacity of SU is analyzed under peak received-power constraint over generalized-K composite fading channels when n PU-Rxs are present. Let g_{pj} represent the channel gain of SU-Tx to j th PU-Rx. Hence, the power constraint is obtained as in [38],

$$g_{pj} P(g_{p1}, g_{p2}, \dots, g_{pn}, g_s) \leq Q_{peak j}, \quad j = 1, 2, \dots, n \quad (4.1)$$

The constraint in (4.1) can be written as,

$$P(g_{p1}, g_{p2}, \dots, g_{pn}, g_s) \leq \min_j \frac{Q_{peak j}}{g_{pj}} \quad (4.2)$$

Furthermore, to simplify the analysis, it can be assumed that $Q_{peak j} = Q_{peak}$, $j = 1, 2, \dots, n$.

4.3.1 Ergodic Capacity

In this section, closed-form expressions of the SU ergodic capacity over shadowed Rayleigh fading channels are derived under the peak received-power (Q_{peak}) constraint of multiple PUs. The ergodic capacity over fading channels assuming full CSI at both the receiver and the transmitter was derived in [38] as,

$$C = \int_{\chi} B \log(1 + \alpha \chi) f_{\chi}(\chi) d\chi \quad (4.3)$$

where $\chi = \frac{g_s}{\max_j g_{pj}}$.

Case I: Rayleigh multipath fading with heavy shadowing for both the SU and the PUs ($m_m=1$, $m_s=0.5$). In this case, for the equivalent Log-normal shadowing model, the dB-spread (σ_{dB}) is 9.1 dB. The PDF of RV χ is derived as (see Appendix B.1),

$$f(\chi) = \frac{n}{2\sqrt{\chi}} \sum_{k=0}^{n-1} (-1)^k \binom{n-1}{k} \frac{1}{(1 + \sqrt{\chi} + k)^2}. \quad (4.4)$$

By substituting $f(\chi)$ from (4.4) in (4.3), the ergodic capacity can be obtained as,

$$C = B n \sum_{k=0}^{n-1} (-1)^k \binom{n-1}{k} \times \frac{\pi\sqrt{\alpha} + \alpha(1+k)(2\log(1+k) + \log(\alpha))}{1 + \alpha(1+k)^2}. \quad (4.5)$$

From Fig. 4.2, the Monte-Carlo simulation and the analytical result of the PDF match each other perfectly.

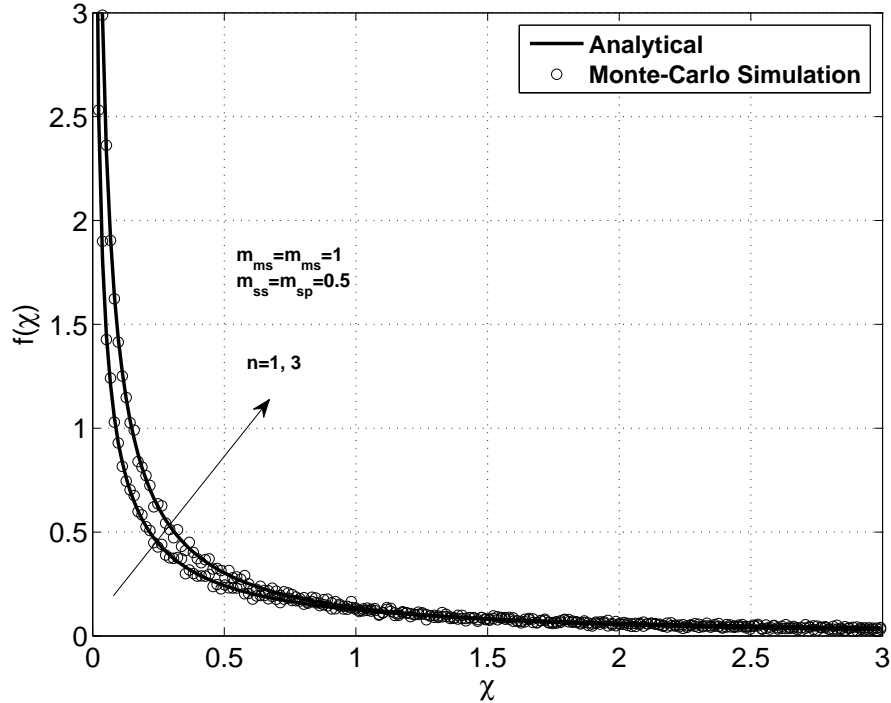


Figure 4.2: Monte-Carlo simulations and analytical results for the $f(\chi)$ of Rayleigh multipath fading with heavy shadowing for different n .

Case II: Rayleigh fading with moderate shadowing ($m_m=1$, $m_s=1.5$) where the dB-spread (σ_{dB}) is 6.2 dB for SU and Rayleigh multipath fading with heavy shadowing for the PUs ($m_s=0.5$). Thus, the PDF can be obtained as (see appendix B.1),

$$f(\chi) = 3n \sum_{k=0}^{n-1} (-1)^k \binom{n-1}{k} \frac{1}{(1 + \sqrt{3}\chi + k)^3}. \quad (4.6)$$

Then, the PDF in (4.6) is used to derive ergodic capacity as in (4.7),

$$\begin{aligned}
C &= B n \sum_{k=0}^{n-1} (-1)^k \binom{n-1}{k} \times \frac{1}{(3 + (1+k)^2 \alpha)^2} \\
&\times \left(6 \pi \sqrt{3 \alpha} - (1+k) \alpha [-6 + (1+k)^2 \alpha (-2 + \log(3)) + 9 \log(3)] \right) \\
&+ (1+k) \alpha (9 + (1+k)^2 \alpha) (2 \log(1+k) + \log(\alpha)).
\end{aligned} \tag{4.7}$$

4.3.2 Outage Probability

Considering an underlay CR networks with multiple PUs, the outage probability for a specific target rate R , $P_{out}(R)$, over fading channels assuming perfect CSI at SU-Tx was derived in [39] as in (3.40).

Case I: Rayleigh multipath fading and heavy shadowing for both the SU and PUs ($m_m=1$, $m_s=0.5$).

The outage probability can be obtained by substituting (4.4) in (3.40), to get,

$$P_{out}(R) = n \sum_{k=0}^{n-1} (-1)^k \binom{n-1}{k} \frac{\sqrt{z}}{(1+)(1+k+\sqrt{z})}. \tag{4.8}$$

Case II: Rayleigh fading with moderate shadowing for SU and Rayleigh multipath fading with heavy shadowing for PUs. Thus, the $P_{out}(R)$ can be derived by substituting (4.6) in (3.40) as,

$$\begin{aligned}
P_{out}(R) &= 3 n \sum_{k=0}^{n-1} (-1)^k \binom{n-1}{k} \times \\
&\frac{z}{(1+k)(3z + (1+k)(1+k+2\sqrt{3z}))}.
\end{aligned} \tag{4.9}$$

4.4 Results and Discussions

In this section, we show and discuss the obtained results for both the ergodic capacity and the outage probability. In Fig. 4.3, the SU's ergodic capacity is depicted for multiple PU-Rxs ($n = 1, 2, 3$) over heavy-shadowed Rayleigh multipath fading channel ($m_{ms} = m_{mp} = 1$ and $m_{ss} = m_{sp} = 0.5$). We see that as the number of PU-Rxs increases, the capacity of the SU decreases as expected.

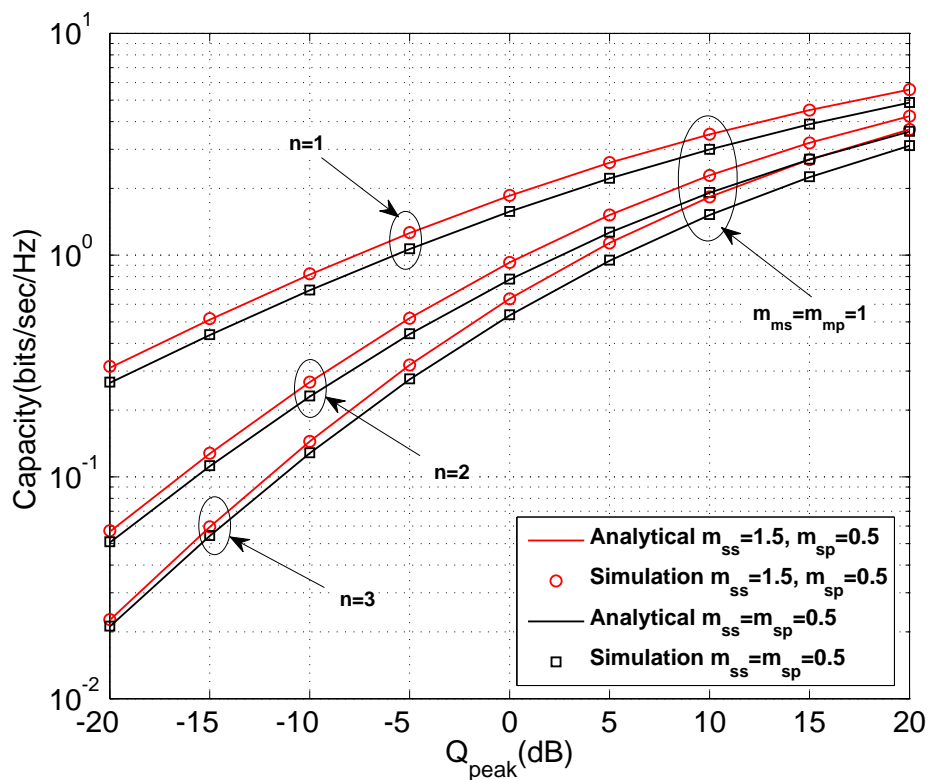


Figure 4.3: Ergodic capacity of SU vs Q_{peak} .

According to Fig. 4.3, the ergodic capacity decreases from 0.4 to 0.05 bits/sec/Hz at -15dB when the number of PUs increases from 1 to 3 for $m_{ms} = m_{mp}=0.5$. In addition, the gain due to shadowing is demonstrated,

however, the relative gain is smaller for $n=3$ due to the higher probability relative to single user scenario, $n = 1$, of having a larger channel gain towards one of the multiple PUs. Furthermore, the analytical results match perfectly with Mont-Carlo simulations.

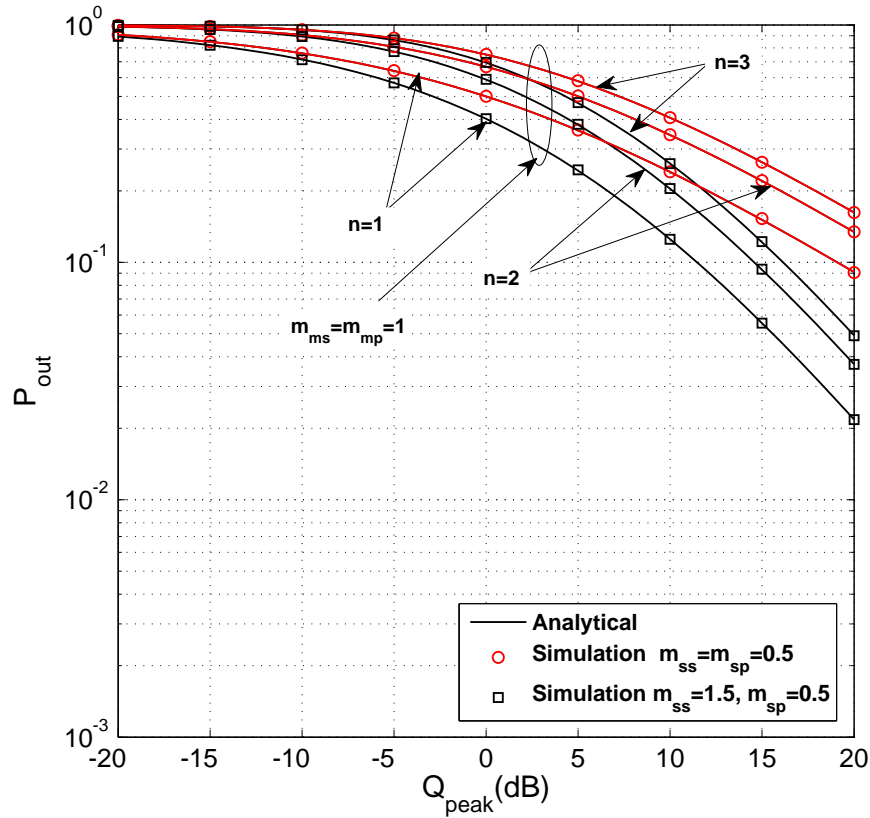


Figure 4.4: The outage probability of the SU with multiple PUs vs Q_{peak} with heavy and moderate shadowing Rayleigh fading channels for the SU.

Figure 4.4 illustrates the outage probability for Rayleigh fading with both heavy and moderate shadowing conditions for the SU and Rayleigh multipath fading with heavy shadowing for the PUs. The target rate is $R = 1$ bit/sec/Hz. It can be seen that the outage probability of Rayleigh fading with moderate shadowing improves as compared to the heavily shadowed

case as expected. The improvement is significant even for $n=1$.

4.5 Conclusions

This chapter considers both the ergodic capacity and outage probability of underlay CR networks over shadowed Rayleigh fading channels under the peak received-power constraint of multiple PUs. In order to evaluate the impact of PUs on the performance of an underly CR networks, we derived closed-form expressions for Rayleigh fading channels with both heavy and moderate shadowing. The obtained results quantified the effect of both multipath fading and shadowing on both the ergodic capacity and outage probability of the SU for different numbers of multiple PUs. Moreover, the effect of a varying number of PUs on the CR performance is investigated as the number of PUs increases, the ergodic capacity declines, and the outage probability rises. Finally, the analytical results are confirmed by using Mont-Carlo simulation.

CHAPTER 5

CAPACITY OF UNDERLAY MULTIHOP COGNITIVE RELAYING

5.1 Introduction

Recently, multi-hop relaying systems are of great interest for achieving a higher data rate coverage demanded in future wireless networks. In addition, they are used to enhance the channels performance. Multi-hop relaying systems consist of multiple serial relays which carry the signals from a source to a destination. As a result of this relaying, the coverage is extended and the transmitted power is reduced at the source which results in lower interference [66]. Relaying techniques are utilized when there is no line of

sight between the source and the destination and the large scale fading or the power constraints affected on the direct transmission. The dual-hop relay system is a simple case of the relaying system where the main purpose of this technique is to relay the forward link into the reverse link. It is used in satellite and microwave communications [66]. Based on the complexity and type of the relays, relayed transmission systems are categorized into two approaches, specifically, AF and DF relays. In the first type, the relays only amplify and forward the received signal without making decoding. In addition, the AF relays are less complex than the DF types. Furthermore, this type of relaying is more beneficial when the transmitted information is more sensitive for the time like live video or voice. In the latter type, the relay decodes the signals which are transmitted from the previous relay and the decoded signal is retransmitted into the following relay. From relay to relay in these systems, the noise vanishes. On the other hand, the error probability increases at each relay.

5.1.1 System and Channel Model

Considering the AF multihop cognitive relaying, the system model consists of an SU-Tx communicating with an SU-Rx by a number of CR relays (N-1) between them as illustrated in Fig. 5.1. For underlay CR, the CR network performs time-division multiple access (TDMA), and the relays are implemented with half-duplex antennas. In this respect, the AF relaying

technique is used in this model. To this end, it is assumed that NLOS link between the SU-Tx and the SU-Rx. Thus, the end-to-end communication is implemented using relays. Furthermore, the communication links are assumed to subject to composite multipath fading. The communication

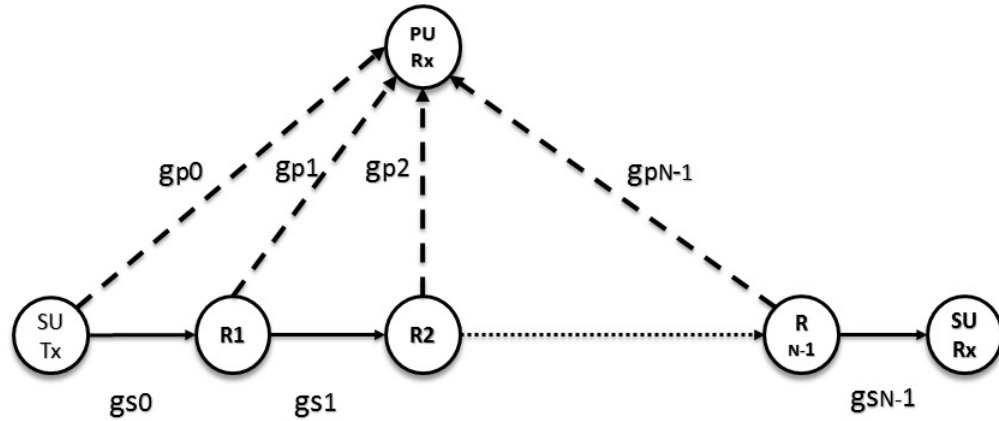


Figure 5.1: System model- multihop cognitive relaying.

between the SUs is achieved under the Q_{peak} , where the SU-Tx and the CR multihop relays have to consider the Q_{peak} at the PU-Rx. Hence, if the transmission power is P_k of the k^{th} terminal, then $P_k g_{pk} \leq Q_{peak}$, and the maximum transmission power can be expressed as $P_k = \frac{Q_{peak}}{g_{pk}}$. Consequently, the end-to-end SNR (γ_{e2e}) at the SU-Rx is obtained in [67] as,

$$\gamma_{e2e} = \left[\sum_{k=1}^N \frac{1}{\gamma_k} \right]^{-1}. \quad (5.1)$$

For the relay R_k , the instantaneous SNR is γ_k where it can be written as $\gamma_k = \frac{Q_{peak} g_{sk}}{N_o g_{pk}}$. However, the γ_{e2e} expression in (5.1) is not mathematically tractable as a result of the lack of a close-form expression of the PDF of the sum in (5.1). Hence, the following upper bound for the γ_k is used [68].

$$\gamma_{e2e} \leq \frac{1}{N} \frac{Q_{peak}}{N_o} \prod_{k=1}^N (X_k)^{\frac{1}{N}} \quad (5.2)$$

Now, the end-to-end upper-bound PDF of the γ_{e2e} is derived. From (5.2), the upper-bound SNR (γ_{e2e}^{up}) is expressed as,

$$\gamma_{e2e}^{up} = \frac{1}{N} \frac{Q_{peak}}{N_o} \prod_{k=1}^N (X_k)^{\frac{1}{N}}. \quad (5.3)$$

where $X_k = \frac{g_{sk}}{g_{pk}}$ are i.i.d. generalized-K RVs, g_s and g_p are two i.n.d. generalized-K RVs. Afterwards, the PDF of the RV $T = \prod_{k=1}^N (X_k)^{\frac{1}{N}}$ can be expressed as,

$$f_T(x) = \frac{N \Psi^N}{\Delta^{N-1}} G_{2N,2N}^{2N,2N} \left((\Delta x)^N \left| \begin{array}{l} (A_1)_1, (A_2)_1, \dots, (A_1)_N, (A_2)_N \\ (A_3)_1, (A_4)_1, \dots, (A_3)_N, (A_4)_N \end{array} \right. \right). \quad (5.4)$$

where $A_1 = -m_{mp} - \frac{1}{N} + 1$, $A_2 = -m_{sp} - \frac{1}{N} + 1$, $A_3 = m_{ms} - \frac{1}{N}$, and $A_4 = m_{ss} - \frac{1}{N}$.

Proof: See Appendix C.1. ■

The obtained theoretical PDF expression is verified by Monte Carlo simulation as shown in Fig. 5.2.

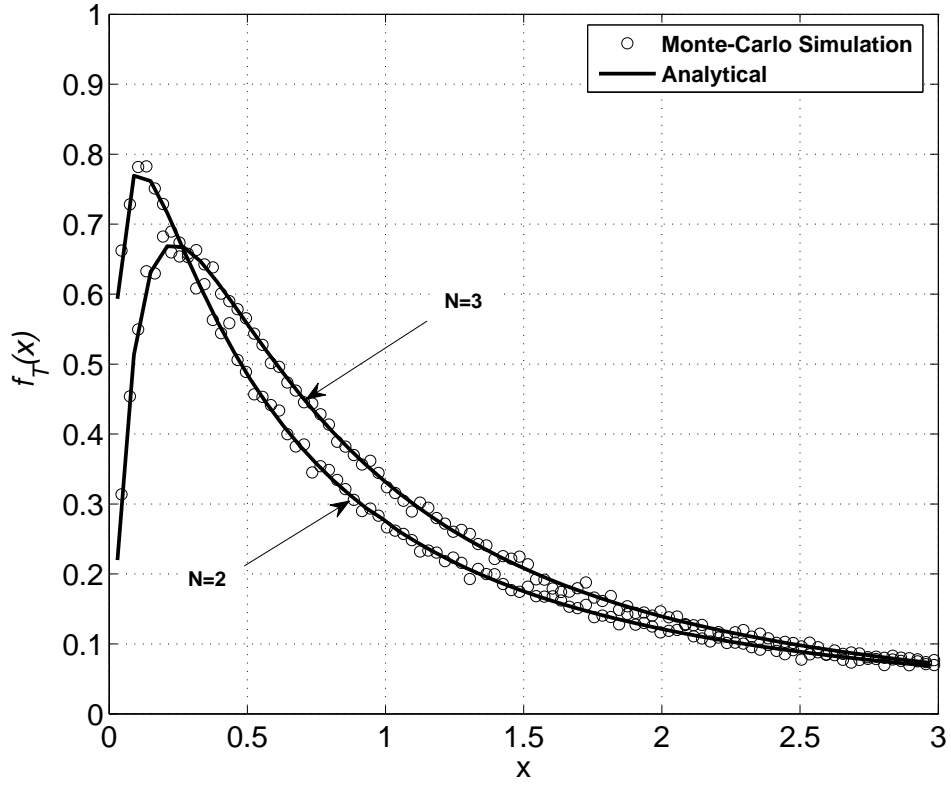


Figure 5.2: Analytical and Monte-Carlo simulation plots for the PDF $f(x)$ of multihop cognitive relaying over composite fading channels for $m_{ms} = m_{mp} = 1$, $m_{ss} = m_{sp} = 2$, $N = 2, 3$.

5.2 Ergodic Capacity

Considering the AF multihop cognitive relaying, the ergodic capacity of the SU is analyzed under peak received-power constraint. However, it is proposed to the systems that are not sensitive to delays. Generally, the ergodic capacity can be expressed as [38],

$$C = B \int_0^{\infty} \log(1 + \alpha x) f_{e2e}(x) dx. \quad (5.5)$$

where $\alpha = \frac{Q_{peak}}{N_o N}$, and $f_{e2e}(x)$ is the end-to-end PDF. Hence, a closed-form expression of an upper bound on the ergodic capacity (C^{up}) can be derived, by substituting (5.4) in (5.5), where $C \leq C^{up}$. For the derivation of the expression in (6.1), the logarithm function is expressed in terms of Meijer G-function as [24, (8.4.6.5)], $\log(1 + \alpha x) = G_{2,2}^{1,2} \left(\alpha x \left| \begin{matrix} 1, 1 \\ 1, 0 \end{matrix} \right. \right)$. As such, the ergodic capacity can be derived by substituting (5.4) in (5.5) as,

$$C \leq C^{up} = B \int_0^\infty G_{2,2}^{1,2} \left(\alpha x \left| \begin{matrix} 1, 1 \\ 1, 0 \end{matrix} \right. \right) \times \frac{N \Psi^N}{\Delta^{N-1}} G_{2N,2N}^{2N,2N} \left((\Delta x)^N \left| \begin{matrix} (A_1)_1, (A_2)_1, \dots, (A_1)_N, (A_2)_N \\ (A_3)_1, (A_4)_1, \dots, (A_3)_N, (A_4)_N \end{matrix} \right. \right) dx \quad (5.6)$$

Thus, for the multihop cognitive relaying over i.n.d. generalized-K composite fading channels, the upper bound on the ergodic capacity is obtained by utilizing the integration formula in [58, (2.24.1.1)]. Hence, the ergodic capacity can be derived as,

$$C^{up} = \frac{B \Psi^N \mu N^{\frac{1}{N}}}{\alpha (2\pi \Delta)^{N-1}} \times G_{4N,4N}^{4N,3N} \left(\frac{\Delta^N}{\alpha^N} \left| \begin{matrix} (A_1)_1, (A_2)_1, \dots, (A_1)_N, (A_2)_N, \Delta(N, -1), \Delta(N, 0) \\ (A_3)_1, (A_4)_1, \dots, (A_3)_N, (A_4)_N, \Delta(N, -1), \Delta(N, -1) \end{matrix} \right. \right). \quad (5.7)$$

where $\alpha = \frac{Q_{peak}}{N_o N}$, $\mu = \sum_{i=1}^N ((A_3)_i + (A_4)_i) - \sum_{i=1}^N ((A_1)_i + (A_2)_i) + 1$ and $\Delta(N, a) = \frac{a}{N}, \frac{a+1}{N}, \dots, \frac{a+N-1}{N}$.

5.3 Outage Probability

The outage probability is considered as a performance metric for delay sensitive applications. In this section, the lower bound on SU outage probability is derived over generalized-K composite fading channels. In this respect, the lower bound of the outage probability (P_{out}^l) for a specific target rate R , $P_{out}^l(R)$, for cognitive multihop relaying can be obtained as,

$$\begin{aligned} P_{out} &\geq P_{out}^l = Pr \left\{ \log_2 \left(1 + \frac{Q_{peak} T}{N_o N} \right) < R \right\} \\ &= Pr \left\{ T < \frac{N N_o (2^R - 1)}{Q_{peak}} \right\}, \end{aligned} \quad (5.8)$$

Let $z = \frac{N N_o (2^R - 1)}{Q_{peak}}$.

Thus, the P_{out}^l can be derived as below,

$$P_{out}^l(z) = \int_z^\infty \frac{N \Psi^N}{\Delta^{N-1}} \times G_{2N,2N}^{2N,2N} \left((\Delta x)^N \left| \begin{array}{l} (A_1)_1, (A_2)_1 \dots (A_1)_N, (A_2)_N \\ (A_3)_1, (A_4)_1 \dots (A_3)_N, (A_4)_N \end{array} \right. \right) dx, \quad (5.9)$$

The integration in (5.9) can be evaluated by using the formula in [58, (2.24.2.2)]. Hence, the P_{out}^l can be obtained as,

$$\begin{aligned} P_{out}^l(z) &= \frac{\Psi^N}{z \Delta^{(N-1)}} \times \\ &G_{3N,3N}^{2N,3N} \left((\Delta z)^N \left| \begin{array}{l} \Delta(N, 0), (A_1)_1, (A_2)_1 \dots (A_1)_N, (A_2)_N \\ (A_3)_1, (A_4)_1 \dots (A_3)_N, (A_4)_N, \Delta(N, -1) \end{array} \right. \right). \end{aligned} \quad (5.10)$$

5.4 Results and Discussion

Considering the AF multihop cognitive relaying, the obtained results and simulations for both ergodic capacity and outage probability are presented in this section. Figure 5.3 depicts the exact and the upper-bounded CR ergodic capacity for AF multihop relaying system. When the number of the relays increases, the ergodic capacity decreases as expected. This is essentially due to the amplification of the additive noise after each AF relay. Also, from Fig. 5.3, the ergodic capacity of the SU increases when the PU link experiences heavy shadowing ($m_{sp} = 0.5$) while the SU link has light shadowing ($m_{ss} = 5$). For both cases, the equivalent dB-spread (σ_{dB}) of the Log-normal shadowing model are 9.1 dB and 3.7 dB. For higher values of Q_{peak} , the exact and the bound curves match.

As illustrated in Fig. 5.4, the ergodic capacity is analyzed for the i.n.d. case where $m_{ms} = m_{mp} = 1$, $m_{ss} = 2$ and different values of the m_{sp} parameter. We can see that the role of m_{sp} parameter (i.e., the shadowing conditions of the PU link) is dominant where the maximum capacity is obtained when the PU link is in heavy shadowing. Furthermore, for the moderate and light shadowing, the effect on the ergodic capacity is similar; however, the heavy shadowing effect is more significant. From figures (5.3) and (5.4), it can be seen that tightness of the bound on the ergodic capacity is better for similar values of both the shadowing and multipath fading parameters of the SU and PU, and small values of N .

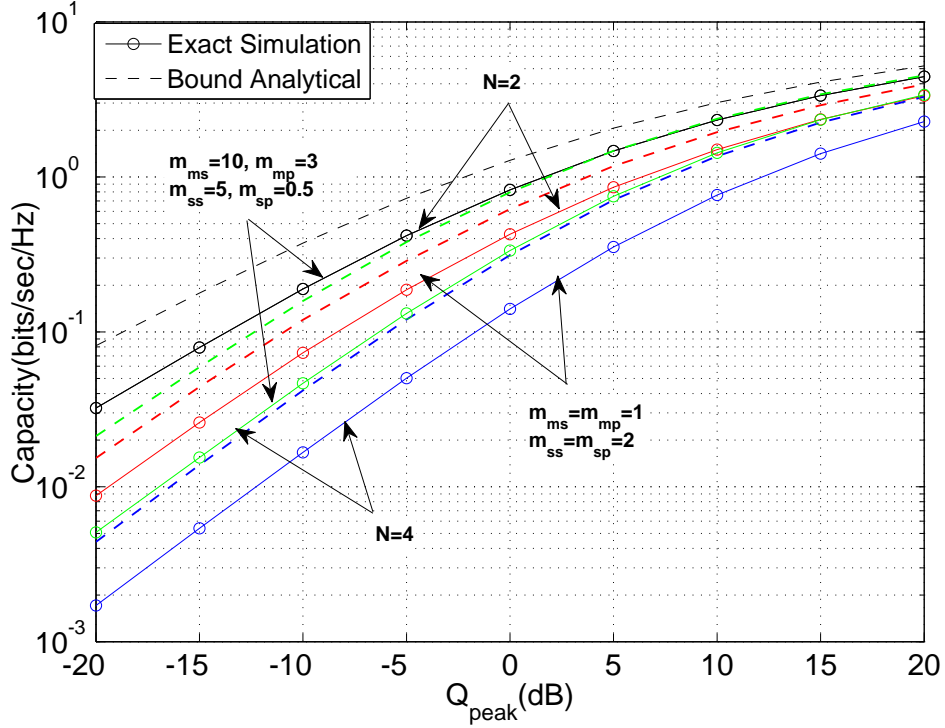


Figure 5.3: Ergodic capacity versus Q_{peak} for $N = 2, 4$.

The outage probability is plotted in Fig. 5.5 for Rayleigh multipath fading with moderate shadowing ($m_{ms} = m_{mp} = 1$, $m_{ss} = m_{sp} = 2$) and $R = 1$ bit/sec/Hz. Furthermore, the outage probability increases with increasing the number of relays as expected.

Figure 5.6 illustrates the outage probability for several scenarios of shadowed Rayleigh fading channels. The obtained result demonstrates the effect of the shadowing parameter m_{ss} of the SU link where the outage probability significantly increases in heavily shadowed environments. Another interesting point is that the bound on the outage probability gets loose due to the difference between the exact PDF/CDF and the approximating one in the lower tail region. However, the lower bound demonstrates the same trend

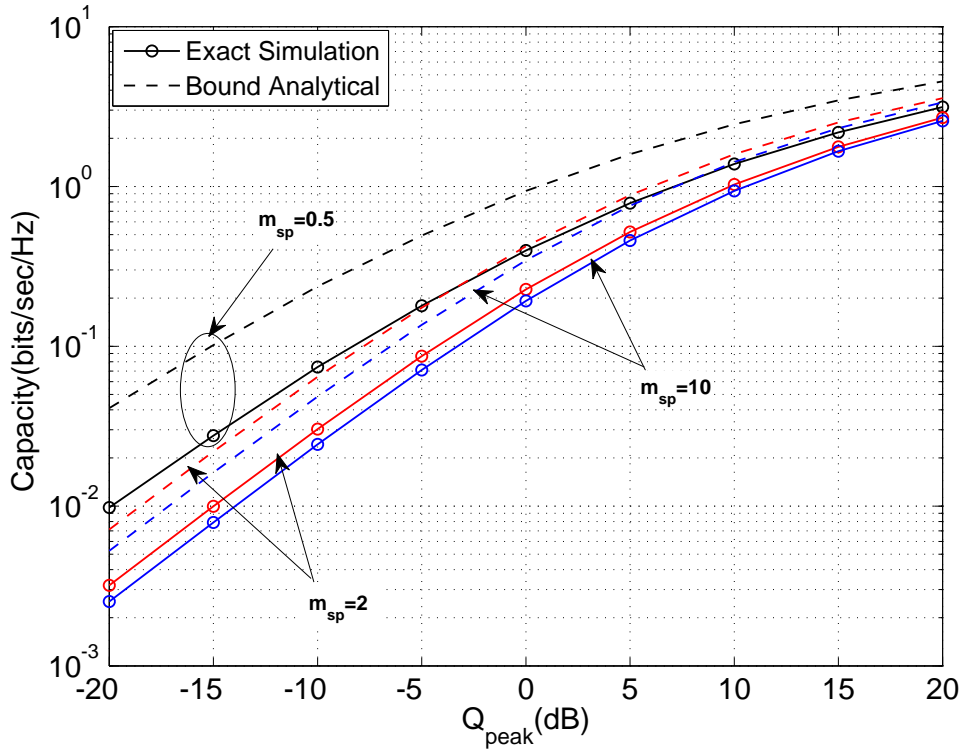


Figure 5.4: The ergodic capacity vs Q_{peak} for different fading and shadowing conditions, $N = 3$.

of the exact results.

5.5 Conclusions

In this chapter, the performance of AF multihop cognitive relaying was analyzed. To do so, an expression for the PDF of the γ_{e2e} was derived and then the derived PDF was utilized to obtain the expressions of the upper and lower bound end-to-end for ergodic capacity and outage probability, respectively. The obtained results quantified the effect of both multipath fading and shadowing on the ergodic capacity and the outage probability,

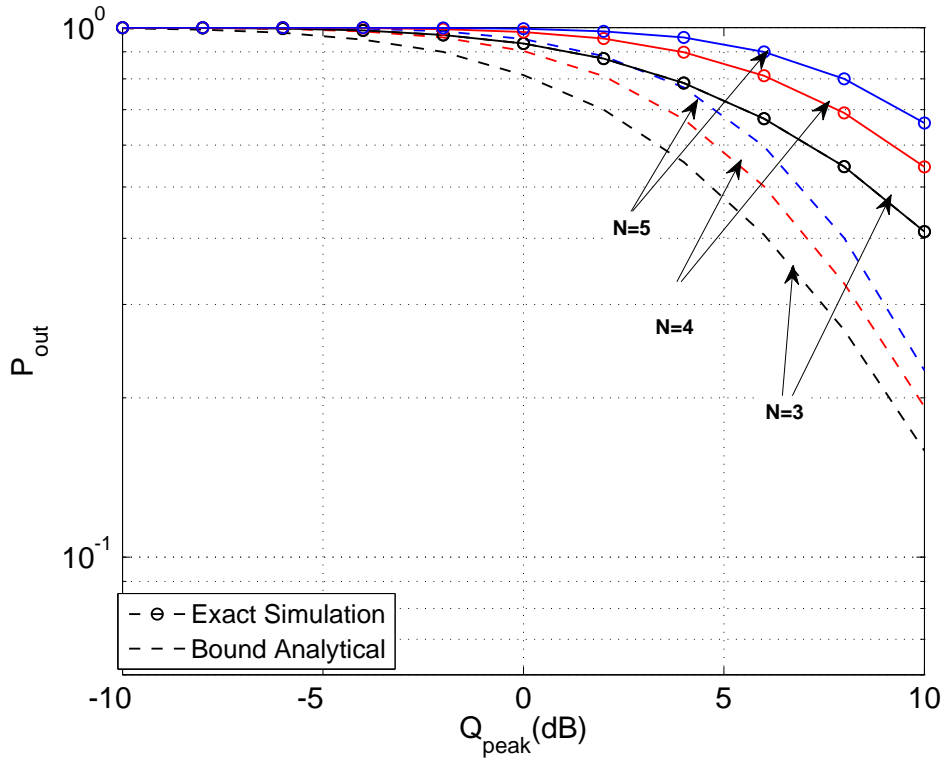


Figure 5.5: The outage probability verse Q_{peak} for different number of relays.

respectively. In addition, the effect of a varying number of AF relays on the CR performance is investigated. As the number of AF relaying increases, the ergodic capacity declines, and the outage probability rises. For comparison purposes, the exact curves are plotted by using Mont-Carlo simulation. Moreover, the analytical results are confirmed by using Mont-Carlo simulation. Furthermore, for the various modulation schemes, the expressions for the average BER can be easily obtained using the derived expressions in this chapter.

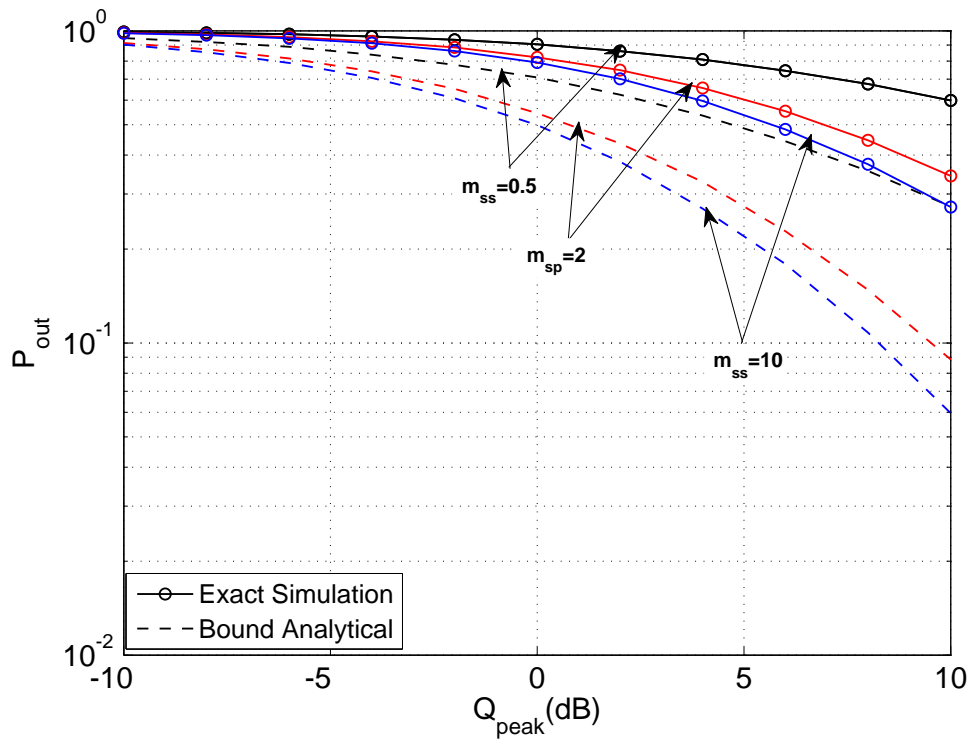


Figure 5.6: The outage probability verse Q_{peak} for different fading conditions and $m_{ms} = m_{mp} = 1$, $m_{sp} = 0.5$, $N = 3$.

CHAPTER 6

CONCLUSIONS AND FUTURE WORK

In this chapter, we conclude the thesis work presented in the previous five chapters including the introduction, background and literature review, capacity of SU with single PU, capacity of SU with multiple PUs, and capacity of cognitive multihop AF relaying. In addition, we propose some interesting topics in cognitive radio capacity to be considered in our future research.

6.1 Conclusions

6.1.1 Capacity of SU with Single PU

In the analysis of the ergodic capacity and outage probability of SU with a single PU, it was found that the ergodic capacity improves due to the

joint effect of both multipath fading and shadowing under both average and peak received-power constraints. To gain more insight, tractable scenarios are investigated in details. In addition, the ergodic capacity under average received power is better than peak received power constraint in the CR networks perspective. From primary networks perspective, the peak power constraints protect the PUs better than average power constraints. Moreover, the effect of both multipath fading and shadowing results in higher outage probability. Furthermore, the approximation of generalized-K distribution is investigated using a single gamma distribution where it matches perfectly with small errors at low SNR. Finally, for Nakagami fading channels, an expression for ergodic capacity is derived with taking the average power constraints into account. In order to verify the analytical results, Mont-Carlo simulations are utilized.

6.1.2 Capacity of SU with Multiple PUs

For more practical platform, the system model in chapter four is extended by including multiple PUs. In this respect, both the ergodic capacity and outage probability of underlay CR networks are analyzed over generalized-K composite fading channels where the peak received-power constraint is taken into account. For interesting cases, namely Rayleigh fading channels with both heavy and moderate shadowing, closed-form expressions are derived. Further insights into the effect of both multipath fading and shadowing on

the CR performance are revealed. Interestingly, the impact of the number of PUs is investigated where CR performance is degrading as the number of PUs increases. Furthermore, the analytical results and the simulations match very well.

6.1.3 Capacity of Cognitive Multihop Relaying

In the analysis of the performance of multihop AF relaying in cognitive radio over generalized-K composite fading channels, the PDF of the product of the rational power of the ratio of two generalized-K RVs is derived. Interestingly, the obtained result is utilized to derive both the upper and lower bound expressions for ergodic capacity and outage probability, respectively. In order to evaluate the impact of multipath fading and shadowing, the analysis examined different fading scenarios. More importantly, the obtained results quantified the effect of the number of relays on the CR performance. To gain more insight, both bounded and exact results were illustrated. In order to confirm the bounded analytical results, Mont-Carlo simulations have shown a perfect match.

6.2 Future Work

There are many open research problems in the capacity of cognitive radio networks over generalized-K composite fading channels that need to be

investigated and evaluated under different system models and parameters. In some extensions of the studied problems in this thesis are proposed as follows:

- Relaying has gained more attraction in the CR networks by reducing the interference and choosing terminals that produce less interference on the PUs. As a result, cognitive relaying is utilized to improve the performance of the CR networks. In this respect, many techniques are used in relay-assisted CR networks such as the best selection relay and multihop relaying. We focused on the cognitive AF multihop relaying. However, the best selection scheme can be utilized to examine the performance of the CR networks over generalized-K composite fading channels. To do so, DF relaying protocol can be used where the best intermediate relaying is chosen to relay the information from SU-Tx to SU-Rx. In doing so, in order to evaluate the impact of SU-Tx and DF Relaying on the PUs, the power constraints is taken into account.
- Cognitive MIMO relaying is considered as a novel framework to cope with spectrum scarcity. From power viewpoint, cognitive MIMO relaying contributes to increasing the reliability of the SUs whereas satisfying power constraints to protect the PUs. Nevertheless, the advantages of cognitive MIMO relaying could be limited by the power constraints. In order to decrease the impact of the restricted power, transmit an-

tenna selection (TAS) is proposed as a novel design managing the interference by using DF relaying. In this respect, two protocols are used, namely TAS with receive selection combining (TAS/SC) and TAS with receive maximal-ratio combining (TAS/MRC). Based on these, the performance of an underlay cognitive MIMO relaying can be investigated to gain more insights into the shadowed multipath environments.

APPENDICES

APPENDIX A

A.1 Ergodic Capacity

Ergodic Capacity - Single PU

The PDF of the quotient in (3.6) reduces to [14, (15)],

$$f_{\frac{g_s}{g_p}}(\chi) = \omega^{m_{ss}} \nu \chi^{m_{ss}-1} \times \left\{ {}_2F_1(m_{ss} + m_{sp}, m_{mp} + m_{ss}; m_{ms} + m_{mp} + m_{ss} + m_{sp}; 1 - \omega \chi) \right\}. \quad (6.1)$$

where $\omega = \left(\frac{m_{ss}m_{ms}}{m_{sp}m_{mp}} \right) \left(\frac{\Omega_{0,p}}{\Omega_{0,s}} \right)$, $\nu = \frac{\beta(m_{mp}+m_{ss}, m_{ms}+m_{sp})}{\beta(m_{ms}, m_{mp})\beta(m_{ss}, m_{sp})}$.

where ${}_2F_1(\cdot, \cdot; \cdot; \cdot)$ represents the Gauss hypergeometric function [24, (9.14)],

and $\beta(\cdot, \cdot)$ denotes the beta function [24, (8.380)]. When $m_{ss} = m_{sp} = m_s$,

$m_{ms} = m_{mp} = m_m$ and $\Omega_{0,p} = \Omega_{0,s} = 1$, (6.1) reduces to,

$$f_{\frac{g_s}{g_p}}(\chi) = \nu \chi^{m_s-1} \times \left\{ {}_2F_1(2m_s, m_m + m_s; 2m_m + 2m_s; 1 - \chi) \right\}. \quad (6.2)$$

For the Rayleigh multipath fading with heavy shadowing channel, $m_m = 1$ and $m_s = 0.5$, the hypergeometric function simplifies to [58, (7.3.3.158)] ,

$${}_2F_1(1, 1.5; 3; 1 - \chi) = \frac{4}{(\sqrt{\chi} + 1)^2}, \quad (6.3)$$

Therefore, the expression in (6.2) reduces as in (3.9).

By substituting (3.9) in both (3.4) and (3.5), the parameter α and the capacity can be obtained as in (3.10) and (3.11), respectively.

For the Rayleigh multipath fading with moderate shadowing channel, $m_m = 1$ and $m_s = 2$, the hypergeometric function simplifies to,

$${}_2F_1(4, 3; 6; 1 - \chi) = \frac{\chi^3 + 9\chi^2 - 3\chi(3 + 2(1 + \chi)\log(\chi)) - 1}{0.1\chi(\chi - 1)^5}, \quad (6.4)$$

Thus, the expression in (6.2) reduces as in (3.12).

By substituting (3.12) in both (3.4) and (3.5), the parameter α and the capacity can be obtained as in (3.13) and (3.14), respectively.

Ergodic Capacity over Nakagami Channels

By substituting (3.19) and (3.5), the α can be obtained as,

$$\frac{1}{\beta(m_m, m_m)} \int_0^{\gamma_0} (\gamma_0 - x) \frac{x^{m_m-1}}{(x+1)^{2m_m}} dx = \alpha,$$

$$\frac{1}{\beta(m_m, m_m)} \left[\int_0^{\gamma_0} \gamma_0 \frac{x^{m_m-1}}{(x+1)^{2m_m}} dx - \int_0^{\gamma_0} \frac{x^{m_m}}{(x+1)^{2m_m}} dx \right] = \alpha,$$

From [24, (3.194.1)], the above integration can be evaluated as in (3.20).

A.2 Outage Probability - Single PU

For the Rayleigh multipath fading with heavy shadowing channel, $m_m = 1$ and $m_s = 0.5$, by substituting (3.9) in both (3.30) and (3.31), we get,

$$P_{out}(R) = 1 - \int_0^y \frac{1}{2\sqrt{\chi}(\sqrt{\chi} + 1)^2} d\chi,$$

and,

$$\int_0^y \frac{\chi}{2\sqrt{\chi}(\sqrt{\chi} + 1)^2} d\chi = \frac{Q_{av}}{N_o(2^R - 1)},$$

Therefore, the $P_{out}(R)$ and y can be obtained as in (3.34) and (3.35), respectively.

For the Rayleigh multipath fading with moderate shadowing channel, $m_m = 1$ and $m_s = 2$, by substituting (3.12) in both (3.36) and (3.37), we get,

$$P_{out}(R) = 1 - \int_0^y \frac{\chi^3 + 9\chi^2 - 3\chi(3 + 2(1 + \chi)\log(\chi)) - 1}{0.5(\chi - 1)^5} d\chi,$$

and,

$$\int_0^y \chi \left(\frac{\chi^3 + 9\chi^2 - 3\chi(3 + 2(1 + \chi)\log(\chi)) - 1}{0.5(\chi - 1)^5} \right) = \frac{Q_{av}}{N_o(2^R - 1)}, \quad (6.5)$$

Thus, the $P_{out}(R)$ and y can be obtained as in (17) and (18), respectively.

APPENDIX B

B.1 PDF Derivations - Multiple PUs

Heavily shadowed Rayleigh fading channels for the SU and PUs

Let g_{pj} ($j = 1, 2, \dots, n$.) be i.i.d. RVs. In addition, we assume that g_s is independent of all g_{pj} . Now, $g_{p,max}$ can be defined as [38],

$$g_p = \max_j g_{pj}, \quad j = 1, \dots, n \quad (6.6)$$

Thus, the CDF of g_p can be expressed as,

$$F_{g_p}(y) = \prod_{j=1}^n F_{g_{pj}}(y),$$

Then, by using the generalized-K CDF expression for integer values of m_m in [69], we may write,

$$F_{g_p}(y) = \left(1 - \frac{2(\Xi y)^{\frac{m_s}{2}}}{\Gamma(m_s)} \sum_{l=0}^{m_m-1} \frac{1}{l!} (\Xi y)^{\frac{l}{2}} K_{m_s-l}(2\sqrt{\Xi y}) \right)^n, \quad (6.7)$$

where $\Xi = m_s m_m / \Omega_0$. Then by substituting $m_s = 0.5$, $m_m = 1$, and $\Omega_0 = 1$ in (6.7) and using $K_{0.5}(z) = \sqrt{\frac{\pi}{2z}} e^{-z}$ [24, (8.469.3)] to get,

$$F_{g_p}(y) = \left(1 - e^{-\sqrt{2y}} \right)^n. \quad (6.8)$$

To find the PDF of g_p , we differentiate (6.8) as,

$$\begin{aligned} f_{g_p}(y) &= \frac{dF_{g_p}(y)}{dy} \\ &= \frac{n e^{-\sqrt{2y}} (1 - e^{-\sqrt{2y}})^{n-1}}{\sqrt{2y}}. \end{aligned} \quad (6.9)$$

Also, the PDF of g_s for $m_m=1$ and $m_s=0.5$ simplifies to,

$$f_{g_s}(x) = \frac{e^{-\sqrt{2x}}}{\sqrt{2x}}. \quad (6.10)$$

Thus, the PDF of $\chi = \frac{g_s}{g_{p,max}}$ can be obtained using [70],

$$\begin{aligned}
f(\chi) &= \int_0^\infty |y| f_{g_s}(y\chi) f_{g_p}(y) dy \\
&= \int_0^\infty |y| \frac{e^{-\sqrt{2y\chi}}}{\sqrt{2y\chi}} \left(\frac{n e^{-\sqrt{2y}} (1 - e^{-\sqrt{2y}})^{n-1}}{\sqrt{2y}} \right) dy \\
&= \frac{n}{2} \sum_{i=0}^{n-1} (-1)^i \binom{n-1}{i} \int_0^\infty \frac{e^{-\sqrt{2y}(1+i+\sqrt{\chi})}}{\sqrt{\chi}} dy
\end{aligned} \tag{6.11}$$

By evaluating the integration in (6.11), the PDF of χ is expressed as in (4.4).

Moderately shadowed Rayleigh fading channel for the SU

For the case when the g_s has the parameters ($m_m = 1$ and $m_s = 1.5$) while the g_{pj} has ($m_m = 1$ and $m_s = 0.5$). By substituting the parameters of g_s in (2.9), the generalized-K PDF reduces to,

$$f_{g_s}(x) = 3 e^{-2\sqrt{1.5x}} \tag{6.12}$$

By substituting (6.12) and (6.9) in (6.11), the PDF of χ for this case is expressed as in (4.6).

APPENDIX C

C.1 PDF Derivations - Multihop Relaying

The PDF of the ratio of the two i.n.d. generalized-K RVs g_s and g_p in X can be given in terms of the Meijer G -function as in (3.6). In addition, by using the upper bound in (5.3), the PDF of the end-to-end SNR can be derived. The PDF of rational power of the ratio of two Generalized-K RVs $Y = X^{\frac{1}{N}}$ can be derived by using [71, Theorem (6.4.2)] as,

$$f_Y(x) = \Psi \Delta^{\frac{1}{N}-1} H_{2,2}^{2,2} \left(\Delta^{\frac{1}{N}} x \left| \begin{array}{c} (-m_{mp} - \frac{1}{N} + 1, \frac{1}{N}), (-m_{sp} - \frac{1}{N} + 1, \frac{1}{N}) \\ (m_{ms} - \frac{1}{N}, \frac{1}{N}), (m_{ss} - \frac{1}{N}, \frac{1}{N}) \end{array} \right. \right) \quad (6.13)$$

where $H_{p,q}^{m,n} \left(x \left| \begin{array}{c} (a_p, c_p) \\ (b_q, c_q) \end{array} \right. \right)$ is the Fox H-function [72, (2.1)]. Furthermore, the PDF of the product of the rational power of X , $T = \prod_{k=1}^N Y_k$, can be obtained by using [71, Theorem (6.4.1)] as,

$$f_T(x) = \frac{\Psi^N}{\Delta^{N-1}} \times H_{2N,2N}^{2N,2N} \left(\Delta x \left| \begin{array}{c} (A_1, \frac{1}{N})_1, (A_2, \frac{1}{N})_1 \dots (A_1, \frac{1}{N})_N, (A_2, \frac{1}{N})_N \\ (A_3, \frac{1}{N})_1, (A_4, \frac{1}{N})_1 \dots (A_3, \frac{1}{N})_N, (A_4, \frac{1}{N})_N \end{array} \right. \right), \quad (6.14)$$

Now, the PDF in (6.14) can be written in terms of Meijer G -function [72] as in (5.4) where it can be simply calculated by using the MATHEMATICA software implementation.

REFERENCES

- [1] V. Valenta, Z. Fedra, R. Maršálek, G. Baudoin, and M. Villegas, “Towards cognitive radio networks: spectrum utilization measurements in suburb environment,” in *Radio and Wireless Symposium, 2009. RWS'09. IEEE*. IEEE, 2009, pp. 352–355.
- [2] B. Wang and K. R. Liu, “Advances in cognitive radio networks: A survey,” *IEEE Journal of Selected Topics in Signal Processing*, vol. 5, no. 1, pp. 5–23, 2011.
- [3] A. Goldsmith, S. A. Jafar, I. Marić, and S. Srinivasa, “Breaking spectrum gridlock with cognitive radios: An information theoretic perspective,” *Proceedings of the IEEE*, vol. 97, no. 5, pp. 894–914, 2009.
- [4] I. F. Akyildiz, W.-Y. Lee, M. C. Vuran, and S. Mohanty, “A survey on spectrum management in cognitive radio networks,” *IEEE Communications Magazine*, vol. 46, no. 4, pp. 40–48, April 2008.
- [5] A. M. Wyglinski, M. Nekovee, and T. Hou, *Cognitive radio communications and networks: principles and practice*. Academic Press, 2010.

- [6] J. Mitola and G. Q. Maguire Jr, “Cognitive radio: making software radios more personal,” *IEEE Personal Communications*, vol. 6, no. 4, pp. 13–18, Aug. 1999.
- [7] S. Haykin, “Cognitive radio: brain-empowered wireless communications,” *IEEE Journal on Selected Areas in Communications*, vol. 23, no. 2, pp. 201–220, Feb. 2005.
- [8] M. K. Simon and M.-S. Alouini, *Digital communication over fading channels, 2nd ed.* John Wiley & Sons, 2005.
- [9] “Spectrum policy task force,” *Federal Commun. Comm., Washington, DC, Rep. ET Docket*, no. 02-135, 2002.
- [10] M. A. McHenry, P. A. Tenhula, D. McCloskey, D. A. Roberson, and C. S. Hood, “Chicago spectrum occupancy measurements & analysis and a long-term studies proposal,” in *Proceedings of The First International Workshop on Technology and Policy for Accessing Spectrum*, Aug. 2006, p. 1.
- [11] T. S. Rappaport *et al.*, *Wireless communications: principles and practice, 2nd ed.* Prentice Hall PTR New Jersey, 2009.
- [12] M. Nakagami, “The m-distribution—a general formula of intensity distribution of rapid fading,” *Statistical Method of Radio Propagation*, 1960.
- [13] A. Abdi and M. Kaveh, “On the utility of gamma pdf in modeling shadow fading (slow fading),” in *IEEE 49th Vehicular Technology Conference*, vol. 3, Jul. 1999, pp. 2308–2312.

- [14] I. Kostić, “Analytical approach to performance analysis for channel subject to shadowing and fading,” *IEE Proceedings-Communications*, vol. 152, no. 6, pp. 821–827, Dec. 2005.
- [15] G. L. Stüber, *Principles of mobile communication, 3rd ed.* Springer Science & Business Media, 2011.
- [16] S. Al-Ahmadi, “The gamma-gamma signal fading model: A survey [wireless corner],” *IEEE Antennas and Propagation Magazine*, vol. 56, no. 5, pp. 245–260, Oct. 2014.
- [17] D. J. Lewinski, “Nonstationary probabilistic target and clutter scattering models,” *IEEE Transactions on Antennas and Propagation*, vol. 31, no. 3, pp. 490–498, 1983.
- [18] P. S. Bithas, N. C. Sagias, P. T. Mathiopoulos, G. K. Karagiannidis, A. Rontogiannis *et al.*, “On the performance analysis of digital communications over generalized-k fading channels,” *IEEE Communications Letters*, vol. 10, no. 5, pp. 353–355, May 2006.
- [19] G. P. Efthymoglou, N. Y. Ermolova, V. Aalo *et al.*, “Channel capacity and average error rates in generalised-k fading channels,” *IET Communications*, vol. 4, no. 11, pp. 1364–1372, Jul. 2010.
- [20] N. Y. Ermolova and O. Tirkkonen, “Outage probability over composite η - μ fading-shadowing radio channels,” *IET communications*, vol. 6, no. 13, pp. 1898–1902, 2012.

- [21] F. Yilmaz and M.-S. Alouini, “A new simple model for composite fading channels: Second order statistics and channel capacity,” in *7th International Symposium on Wireless Communication Systems (ISWCS)*, Sept. 2010, pp. 676–680.
- [22] J. Anastasov, G. T. Djordjevic, M. C. Stefanovic *et al.*, “Analytical model for outage probability of interference-limited systems over extended generalized-k fading channels,” *IEEE Communications Letters*, vol. 16, no. 4, pp. 473–475, April 2012.
- [23] S. Al-Ahmadi and H. Yanikomeroglu, “On the approximation of the generalized-k distribution by a gamma distribution for modeling composite fading channels,” *IEEE Transactions on Wireless Communications*, vol. 9, no. 2, pp. 706–713, Feb. 2010.
- [24] I. S. Gradshteyn and I. M. Ryzhik, *Table of integrals, series, and products, 7th ed.* Academic Press, 2007.
- [25] H. Tabassum, Z. Dawy, E. Hossain, and M.-S. Alouini, “Interference statistics and capacity analysis for uplink transmission in two-tier small cell networks: A geometric probability approach,” *IEEE Transactions on Wireless Communications*, vol. 13, no. 7, pp. 3837–3852, July, 2014.
- [26] A. Goldsmith, *Wireless communications.* Cambridge university press, 2005.
- [27] C. E. Shannon, “Communication theory of secrecy systems,” *Bell system technical journal*, vol. 28, no. 4, pp. 656–715, 1949.

- [28] D. Tse and P. Viswanath, *Fundamentals of wireless communication*. Cambridge university press, 2005.
- [29] R. Zhang, “On peak versus average interference power constraints for protecting primary users in cognitive radio networks,” *IEEE Transactions on Wireless Communications*, vol. 8, no. 4, pp. 2112–2120, April 2009.
- [30] H. Urkowitz, “Energy detection of unknown deterministic signals,” *Proceedings of the IEEE*, vol. 55, no. 4, pp. 523–531, April 1967.
- [31] F. F. Digham, M.-S. Alouini, and M. K. Simon, “On the energy detection of unknown signals over fading channels,” *IEEE Transactions on Communications*, vol. 55, no. 1, pp. 21–24, Jan. 2007.
- [32] Y. Zeng, C. L. Koh, and Y.-C. Liang, “Maximum eigenvalue detection: theory and application,” in *IEEE International Conference on Communications, 2008. ICC’08.*, May 2008, pp. 4160–4164.
- [33] J. Ma, G. Y. Li, and B. H. F. Juang, “Signal processing in cognitive radio,” *Proceedings of the IEEE*, vol. 97, no. 5, pp. 805–823, May 2009.
- [34] L. Luo, N. M. Neihart, S. Roy, and D. J. Allstot, “A two-stage sensing technique for dynamic spectrum access,” *IEEE Transactions on Wireless Communications*, vol. 8, no. 6, pp. 3028–3037, June 2009.
- [35] S. Maleki, A. Pandharipande, and G. Leus, “Two-stage spectrum sensing for cognitive radios,” in *IEEE International Conference on Acoustics Speech and Signal Processing (ICASSP)*, Mar. 2010, pp. 2946–2949.

- [36] A. J. Goldsmith and P. P. Varaiya, “Capacity of fading channels with channel side information,” *IEEE Transactions on Information Theory*, vol. 43, no. 6, pp. 1986–1992, Nov. 1997.
- [37] M. Gastpar, “On capacity under receive and spatial spectrum-sharing constraints,” *IEEE Transactions on Information Theory*, vol. 53, no. 2, pp. 471–487, Feb. 2007.
- [38] A. Ghasemi and E. S. Sousa, “Fundamental limits of spectrum-sharing in fading environments,” *IEEE Transactions on Wireless Communications*, vol. 6, no. 2, pp. 649–658, Feb. 2007.
- [39] X. Kang, Y.-C. Liang, A. Nallanathan, H. K. Garg, and R. Zhang, “Optimal power allocation for fading channels in cognitive radio networks: Ergodic capacity and outage capacity,” *IEEE Transactions on Wireless Communications*, vol. 8, no. 2, pp. 940–950, Feb. 2009.
- [40] L. Musavian and S. Aïssa, “Capacity and power allocation for spectrum-sharing communications in fading channels,” *IEEE Transactions on Wireless Communications*, vol. 8, no. 1, pp. 148–156, Jan. 2009.
- [41] G. Noh, S. Lim, and D. Hong, “Exact capacity analysis of spectrum sharing systems: Average received-power constraint,” *IEEE Communications Letters*, vol. 17, no. 5, pp. 884–887, May 2013.
- [42] C.-X. Wang, X. Hong, H.-H. Chen, and J. Thompson, “On capacity of cognitive radio networks with average interference power constraints,”

- IEEE Transactions on Wireless Communications*, vol. 8, no. 4, pp. 1620–1625, April 2009.
- [43] S. Sridharan and S. Vishwanath, “On the capacity of a class of mimo cognitive radios,” *IEEE Journal of Selected Topics in Signal Processing*, vol. 2, no. 1, pp. 103–117, Feb. 2008.
- [44] Y. J. A. Zhang and A.-C. So, “Optimal spectrum sharing in mimo cognitive radio networks via semidefinite programming,” *IEEE Journal on Selected Areas in Communications*, vol. 29, no. 2, pp. 362–373, Feb. 2011.
- [45] R. Zhang, F. Gao, and Y.-C. Liang, “Cognitive beamforming made practical: Effective interference channel and learning-throughput trade-off,” *IEEE Transactions on Communications*, vol. 58, no. 2, pp. 706–718, Feb. 2010.
- [46] S. Akin and M. C. Gursoy, “Performance analysis of cognitive radio systems under qos constraints and channel uncertainty,” *IEEE Transactions on Wireless Communications*, vol. 10, no. 9, pp. 2883–2895, Sept. 2011.
- [47] E. C. Van Der Meulen, “Three-terminal communication channels,” *Advances in applied Probability*, pp. 120–154, 1971.
- [48] A. Sendonaris, E. Erkip, and B. Aazhang, “User cooperation diversity. part i. system description,” *IEEE Transactions on Communications*, vol. 51, no. 11, pp. 1927–1938, Nov. 2003.

- [49] G. Kramer, M. Gastpar, and P. Gupta, “Cooperative strategies and capacity theorems for relay networks,” *IEEE Transactions on Information Theory*, vol. 51, no. 9, pp. 3037–3063, Sept. 2005.
- [50] S. Song, K. Son, H.-W. Lee, and S. Chong, “Opportunistic relaying in cellular network for capacity and fairness improvement,” in *IEEE Global Telecommunications Conference, (GLOBECOM’07)*, Nov. 2007, pp. 4407–4412.
- [51] K. Ben Fredj, L. Musavian, and S. Aïssa, “Closed-form expressions for the capacity of spectrum-sharing constrained relaying systems,” in *IEEE 17th International Conference on Telecommunications (ICT), 2010*, April 2010, pp. 476–480.
- [52] K. B. Fredj, S. Aïssa, and L. Musavian, “Ergodic and outage capacities of relaying channels in spectrum-sharing constrained systems,” *IET Communications*, vol. 7, no. 2, pp. 98–109, April 2013.
- [53] X. Zhang, Y. Zhang, Z. Yan, J. Xing, and W. Wang, “Performance analysis of cognitive relay networks over nakagami-m fading channels,” *IEEE Journal on Selected Areas in Communications*, vol. 33, no. 5, pp. 865–877, May 2015.
- [54] J. Hussein, S. Ikki, S. Boussakta, C. Tsimenidis, and J. Chambers, “Performance analysis of a multi-hop ucrn with co-channel interference,” *IEEE Transactions on Communications*, vol. 64, no. 10, 2016.

- [55] P. S. Bithas, G. P. Efthymoglou, and D. S. Kalivas, “Outage probability of cognitive relay networks over generalized fading channels with interference constraints,” *Procedia Computer Science*, vol. 40, pp. 84–91, 2014.
- [56] G. N KAMGA, K. Ben Fredj, and S. Aissa, “Multihop cognitive relaying over composite multipath/shadowing channels,” *IEEE Transactions on Vehicular Technology*, vol. 64, no. 8, pp. 3807–3812, Aug. 2015.
- [57] N. Miridakis, “On the ergodic capacity of underlay cognitive dual-hop af relayed systems under non-identical generalized-k fading channels,” *IEEE Early Access Articles*, 2015.
- [58] Y. A. Brychkov, O. Marichev, and A. Prudnikov, “Integrals and series, vol 3: more special functions,” *Gordon and Breach science publishers*, 1986.
- [59] N. L. Johnson and S. Kotz, *Distributions in Statistics: Continuous Univariate Distributions: Vol.: 2*. Houghton Mifflin, 1970.
- [60] H. Tran, T. Q. Duong, and H.-J. Zepernick, “Performance analysis of cognitive relay networks under power constraint of multiple primary users,” in *Global Telecommunications Conference (GLOBECOM 2011)*. IEEE, 2011, pp. 1–6.
- [61] T. Q. Duong, P. L. Yeoh, V. N. Q. Bao, M. ElKashlan, and N. Yang, “Cognitive relay networks with multiple primary transceivers under

- spectrum-sharing,” *IEEE Signal Processing Letters*, vol. 19, no. 11, pp. 741–744, 2012.
- [62] T. Q. Duong, K. J. Kim, H.-J. Zepernick, and C. Tellambura, “Opportunistic relaying for cognitive network with multiple primary users over nakagami-m fading,” in *IEEE International Conference on Communications (ICC)*. IEEE, 2013, pp. 5668–5673.
- [63] H. Huang, Z. Li, J. Si, and L. Guan, “Underlay cognitive relay networks with imperfect channel state information and multiple primary receivers,” *IET Communications*, vol. 9, no. 4, pp. 460–467, 2014.
- [64] A. Hyadi, M. Benjillali, M.-S. Alouini, and D. B. da Costa, “Performance analysis of underlay cognitive multihop regenerative relaying systems with multiple primary receivers,” *IEEE Transactions on Wireless Communications*, vol. 12, no. 12, pp. 6418–6429, 2013.
- [65] A. M. Salhab and S. A. Zummo, “Spectrum-sharing of relay networks with switch-and-examine relaying and multiple primary users using orthogonal spectrums,” *Arabian Journal for Science and Engineering*, vol. 41, no. 2, pp. 1–13, 2015.
- [66] M. Guizani, *Wireless communications systems and networks*. Springer Science & Business Media, 2006.
- [67] M. O. Hasna and M.-S. Alouini, “End-to-end performance of transmission systems with relays over rayleigh-fading channels,” *IEEE Transactions on Wireless Communications*, vol. 2, no. 6, pp. 1126–1131, 2003.

- [68] G. K. Karagiannidis, T. A. Tsiftsis, and R. K. Mallik, “Bounds for multihop relayed communications in nakagami-m fading,” *IEEE Transactions on Communications*, vol. 54, no. 1, pp. 18–22, 2006.
- [69] G. P. Efthymoglou, “On the performance analysis of digital modulations in generalized-k fading channels,” *Wireless Personal Communications*, vol. 65, no. 3, pp. 643–651, 2012.
- [70] A. Papoulis and S. U. Pillai, “Probability, random variables, and stochastic processes,” *McGraw-Hill*, 2002.
- [71] M. D. Springer, *The algebra of random variables*. John Wiley & Sons, 2009.
- [72] A. M. Mathai, R. K. Saxena, and H. J. Haubold, *The H-function: theory and applications*. Springer Science & Business Media, 2009.

Vitae

- Name: Majid Hamoud Ahmed Khoshafa
- Nationality: Yemeni
- Date of Birth: 1982
- Email: *eng.khoshafa@gmail.com*
- Permenant Address: Ibb, Yemen

Publications

Journal Papers

1. Majid H. Khoshafa and Saad AL-Ahmadi. “On the Capacity of Underlay Cognitive Radio Networks over Generalized-K Composite Fading Channels.” submitted to *Arabian Journal for Science and Engineering* (2016).
2. Majid H. Khoshafa and Saad AL-Ahmadi. “On the Capacity of Underlay Multihop Cognitive Relaying over Shadowed Multipath Fading Channels.” submitted to *Wireless Personal Communications* (2016).